



**KTH Industrial Engineering
and Management**

Development of a heat treatment method to form a duplex microstructure of lower bainite and martensite in AISI 4140 steel

Erik Claesson

Master Thesis

Department of Material Science and Engineering
Royal Institute of Technology
Stockholm, Sweden
2014

By: Erik Claesson

Degree project report at

Degree Program in Materials Design and Engineering

Royal Institute of Technology, KTH, Stockholm

Supervisor: Lisa Earnest

Cummins Fuel Systems

Cummins Inc, 1460 N National Rd, Columbus, IN 47201

Examiner: Prof. Joakim Odqvist

Department of Metallography, School of Industrial Engineering and

Management, Royal Institute of Technology, KTH, Stockholm

June 2014

Abstract

Research on bainite and martensite structures has indicated that lower bainite needles have a refining effect on the lath martensitic structure. Lower bainite needles partition prior austenite grains and will consequently have a refining effect on the subsequently formed lath martensite. Smaller austenite grains will result in smaller lath martensitic packets and blocks and will result in enhanced mechanical properties.

In order to create a variation of lower bainite structure in a matrix of martensite, two different heat treating methods were tested. The work was focused towards the formation of lower bainite during isothermal heat treating in molten salt, above and below the M_s -temperature. Both untempered and tempered samples were analyzed. Two different materials were tested, both were AISI 4140 but with a slightly difference in hardenability. The material provided by Ovako Steel is 326C and 326F the later had a higher hardenability.

In order to better distinguish the two structures from each other when studied under a microscope, a variation of etching methods were tested.

It was possible to create a variation of lower bainite structures in a matrix of martensite. 326F shows less amount of lower bainite and provides a higher average surface hardness before tempering.

Keywords: AISI 4140, 326C, 326F, Isothermal heat treatment, Martensite, Bainite, Molten salt, vacuum furnace, gas quenching.

Sammanfattning

Forskning på mikrostrukturer med en kombination av bainit och martensit har visat att underbainit har en förfinande effekt på den martensitiska strukturen. De underbainitiska nålarna delar upp de austenitiskakornen, vilket leder till den latt-martensitiska understrukturen blir finare. Den förfinande strukturen resulterar i högre mekaniska egenskaper.

För att skapa olika halter av underbaint in en matris av martensit, testades olika värmebehandlingar. Arbetet fokuserades mot underbaintisk formation under isotermiskvärmebehandling i smalt salt. Två olika temperaturer av isotermiskvärmebehandling testades, över och under M_s . Även med eller utan ett avslutande anlöpnings steg testades. Två olika material undersöktes bada AISI 4140 men med skillnad hårdbarhet. Materialen från Ovako Steel AB heter 326C och 326F, den senare hade en högre hårdbarhet.

For att skilja martensit och bainte från varandra när de studeras under ett mikroskop testades också olika etsnings metoder for att bättre kunna skilja underbaint och martesnite från varandra.

Det var möjligt att skapa olika halter av underbaint i martensit. Material 326F förenklade bainit formationen samt att den gav en högre genomsnittlig hårdhet före anlöpning.

Nyckelord: AISI 4140, 326C, 326F, Isotermisk värmebehandling, Martensit, Bainit, salt, vakuum ugn, gas släckning

Acknowledgement

This work has been a co-operation between Cummins Fuel Systems and the Royal Institute of technology (KTH) in Stockholm, but also a part of my time at Purdue University. The work was conducted at the Cummins Fuel Systems Plant in Columbus Indiana, during the spring of 2014.

First of all I would like to thank everybody at the Material Engineering department at Cummins Fuel Systems in Columbus Indian, USA, for this great opportunity.

A big thanks to Lisa Earnest who helped me to get a better understanding about the fuels systems business and who gladly answered all my questions. I would like to show great appreciation to Madeline Fogler for the feedback and guidance during the whole project and for the general help with the writhing of the thesis.

Charles Thomas helped me with the practical work and with his great knowledge about heat treating processes provided me with a lot of interesting and necessary information to bring this work forward, for which I am grateful.

Thanks to Terry Parsons and the technicians at the material engineering department at Cummins Fuel systems for helping me with practical work, analyzing the samples.

I would like to thank Dr. Joakim Odquist who was my supervisor at the KTH for his guidance and the feedback he provided during the whole period.

Erik Claesson

Columbus Indiana, USA, May, 2014

Nomenclature

M_S	Martensitic start temperature
M_F	Martensitic finish temperature
FCC	Face central cubic
BCC	Body central cubic
BCT	Body central tetragonal
σ	Tensile strength
LOM	Light optical Microscope
SEM	Secondary electron Microscopy
XRD	X-ray diffraction
σ_y	Total strength of lath martensite
σ_0	Friction stress for pure iron
σ_p	Precipitation hardening
σ_s	Solidification hardening
σ_p	dislocation hardening
$K_{HPd}^{1/2}$	Grain boundary strength, hall petch
W_{LB}	Width of Lower Bainite Needle
L_{LB}	Length of Lower Bainite Needle
S_{UM}	Martensite size
S_{UB}	Upper Bainite size
$\sigma_{0.2}^{mix}$	Yield strength of mixed structure
$\sigma_{0.2}^M$	Yield strength Martensite
$\sigma_{0.2}^B$	Yield strength Bainite
V_B	Bainite Volume
S_M	Martensite Packet size

k	Constant
σ_i	Friction stress
T _a	Arrest temperature, for marentsite transformation
EBSD	Electron backscattering diffraction

Table of Contents

1. Introduction.....	1
1.1. Aim of the present work	2
2. Background	3
2.1. Martensite	3
2.1.1. Kinetics of martensite formation	4
2.2. Formation of Bainite	7
2.2.1. Diffusionless growth.....	8
2.2.2. Diffusional growth.....	9
2.3. Upper and lower bainite.....	10
2.4. Combination of Martensite and Bainite	13
2.5. Banded structures	18
2.6. Heat treating.....	21
2.6.1. Quenching	22
2.6.2. Oil quenching	23
2.6.3. Gas quenching.....	23
2.6.4. Molten salt quenching.....	24
2.6.5. Isothermal heat treating temperature	25
2.7. AISI 4140	25
2.8. Etching	26
2.9. Point Counting Method	27
3. Materials	28
4. Experimental procedures	30
4.1. Sample preparation.....	30
4.2. Sample analysis.....	30
4.3. Heat treatment	32
4.4. Etching methods	33
5. Result and Discussion.....	34
5.1. Vacuum heating gas quenching (VHGQ)	34
5.1.1. VHGQ test 1	34
5.2. Austempering in molten salt	36

5.2.1. Trial A.....	36
5.2.2. Isothermal heat treating temperature.....	40
5.2.3. Trial B.....	41
5.2.4. Comparison of data.....	44
5.3. Etching methods.....	48
6. Conclusions.....	52
7. Further work.....	52
References.....	53

1. Introduction

In the fuel system industry the production of materials with high mechanical properties *i.e.* strength and hardness, is crucial in order to provide the customers with reliable products. The everyday work at the Materials department at Cummins Fuel Systems involves solving problems caused by heat treatment issues, rust, manufacturing defects or steel making defects. Everything from cracks caused by inclusions to failures due to manufacturing problems are being analyzed, and solved.

The fuel systems designed and manufactured in Columbus, Indiana consist of 6 or 8 fuel injectors, a fuel pump and a rail connecting the pump and the injectors. The highly calibrated and sensitive technology relies on material made to withstand high cyclic pressure for one million miles on engine. A primary component in the injector is the injector body made from AISI 4140 (Ovako 326C) steel provided from Ovako AB. Research in order to understand the different parameters *i.e.* heat treatment, machining and finishing operations is important. Knowledge about materials and the operating environments will aid the development of new materials with better mechanical properties. Knowledge to further understand the impact of the microstructural result of steel heat treatment is something that has been investigated for a long time, with a high focus on the austenite transformation and its products. The formation and distribution of microstructures in steels will very much influence the limitations of the product.

The transformation of austenite into non-martensitic structures is often related to insufficient heat treatment. The heat treating process has been developed to ensure no non-martensitic transformation products and thereby desired properties. Problems have occurred due to the difficulties to control heat treating to produce 100% martensite structure. However, it has been shown that non-martensitic transformation into lower bainite can increase the mechanical properties. Lower bainite is a fine and complex structure of ferrite and cementite, and have shown to increase toughness, strength and fatigue properties.

For many years, AISI 4140 has been heat treated to form a martensitic structure. The characteristics of tempered martensite have been favorable when it comes to high demanding applications. Tempered martensite has been used for its excellent mechanical properties in applications where it is important to withstand high pressure fatigue environments. However, problems involving distortion and micro cracking in the structure can lower the fatigue strength. A duplex structure of martensite and lower bainite has shown to increase the tensile strength. [1] Indications that the fatigue strength also can be increased with a combination of martensite and lower bainite has raised the motivation to further research this phenomenon. [2] [3] [4] [5]

1.1. Aim of the present work

This work is considered a pre-study before mechanical testing. Cummins and Ovako are teaming up to further investigate AISI 4140 with mixed levels of bainite and martensite.

The main objective is to heat treat AISI 4140 in order to form different levels of bainite, measure the bainite content by using a point counting method, and use a variation of etchants to better distinguish bainite and martensite.

Two different materials with slightly different hardenability levels will be shipped to a heat treat supplier in order to perform isothermal heat treatment in a molten salt bath. This will form a variation of bainite levels in a martensite matrix.

The vacuum harden and gas quench furnace at Cummins Fuel Systems in Columbus, Indiana will be used in order to try to adjust the cooling rate to form bainite. Parameters such as pressure, with or without use of a cooling fan, section size and variation in atmosphere will decide the resulting microstructure.

2. Background

2.1. Martensite

Many materials form a martensitic structure by quenching. However, the diffusionless formation of martensite is most associated with steel processing and rapid transformation of austenite. The formation of martensite is highly influenced by the carbon content, prior austenite grain size and the alloy content. All three parameters are also associated with steel hardenability.

The diffusionless transformation from austenite and the high strength of martensite are related to trapped carbon atoms in the martensite lattice. Since diffusion does not have time to occur, the chemical composition and distribution of alloying elements in the formed martensite is determined by the converted austenite. The maximum carbon content in austenite is around 2%, since martensite only can be formed via austenite transformation, 2% is also the maximum carbon content in martensite. The austenite face centered cubic (FCC) lattice will upon quenching transform into martensite body centered tetragonal (BCT) lattice via a shear mechanism, resulting in trapped carbon atoms. The shear mechanism affects the lattice and causes the surface to tilt, which results in plastically deformed regions close to the tilted surface as shown in Figure 1. [6]

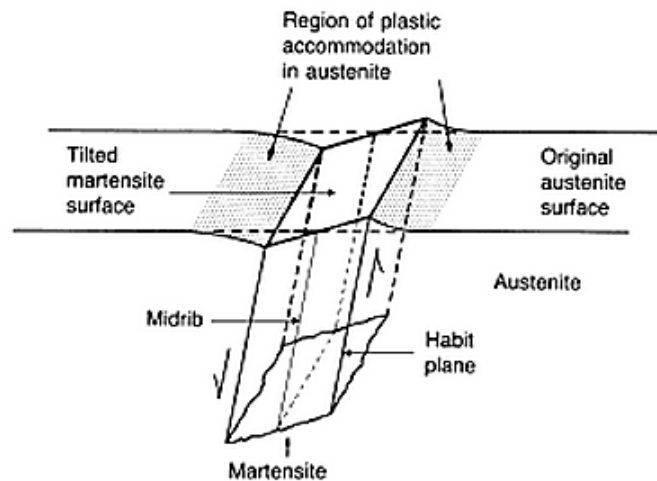


Figure 1. Schematic picture of the martensitic shear mechanism resulting in a tilted martensite surface [6]

The habit plane is the preferred austenite plane from which the martensite crystals are nucleated. The interface between the two phases is ideally planar, but varies with composition. The plane where the formation is initiated is called the midrib. The midrib is a characteristic feature for the martensitic phase, when studied under a microscope the midrib can be seen as a line in the center of the martensitic phase dividing it in half. The formation of martensite is due to a displacive formation. Instead of diffusion in order to adapt to the new lower energy state at lower temperature, the carbon atoms are moved simultaneously by the shear mechanism, in opposite

direction on each side of the midrib plane. The forced displacement of carbon atoms will result in high amount of internal stresses and an increase in dislocation density, resulting in a hard but brittle material. [6]

In contrast to the ferrite body centered cubic (BCC) lattice, the martensitic BCT lattice has one side that is longer than the other two sides, resulting in more interstitial sites, and a higher solubility of carbon.

Martensite is a metastable phase that will decompose into ferrite and carbides (depending on carbon content) during tempering. The decomposition of martensite during tempering can be divided into the following steps:

1. Formation of carbides, resulting in decreased carbon content in the martensitic structure, which will decrease the residual stresses. The carbides are a so-called transition carbides named epsilon
2. If any retained austenite is present it will decompose into ferrite and carbides
3. Decomposition of martensite into ferrite and carbides

The time necessary for decomposition depends on the temperature, and the mobility of the carbon atoms. [6]

2.1.1. Kinetics of martensite formation

The diffusionless transformation is an athermal transformation because it is not associated with any thermal activation. When cooled below the martensitic start temperature (M_S), the formation of martensite will take place. Theoretically, if the temperature is cooled down and kept at a certain temperature under M_S but above the martensitic finish temperature (M_F), for a long time, no further formation of martensite will take place. M_F is the temperature when the last transformation of austenite into martensite occurs. The M_S and M_F are related to the amount of driving force for martensite transformation, which is the energy needed for the shear mechanism to take place. The M_S depends on the carbon content in the steel. Alloys with higher carbon content will have a lower corresponding M_S . Hence, higher carbon content provides higher resistance against transformation into martensite. The amount of alloying elements will also have a decreasing effect on the M_S and M_F . In general, alloying elements will lower the M_F with the exception of cobalt. Different equations have been established over the years to describe the impact of alloying elements on M_S and M_F , and are further described by George Krauss. [6]

When the carbon content reaches 0.3wt% and above, M_F will go below room temperature, increasing the risk for retained austenite. Retained austenite impairs the mechanical properties

and is not desired in Fuel Systems products. In order to ensure that no austenite will remain in the steel after quenching, deep freezing is commonly used *i.e.* in liquid nitrogen. [6]

The carbon content also decides what type of martensite that will be formed. Two variations of martensite exist, lath and plate martensite. An increase in carbon content will lower the M_S and M_F temperatures. However, increasing the carbon content will consequently lead to a difference in the appearance of martensite, as shown in Figure 2. Lath martensite is formed at lower carbon levels while plate martensite is formed at higher levels. Lath and plate martensite are three-dimensional individual crystals of martensite. When etched and studied under a microscope, lath and plate martensite can be seen as needles or acicular plates respectively. However, the microstructure is often too fine to see any of the needles or the acicular crystals in light optical microscope. Bainite has a similar appearance and is one reason that these two structures can be difficult to distinguish in a light optical microscope. [6]

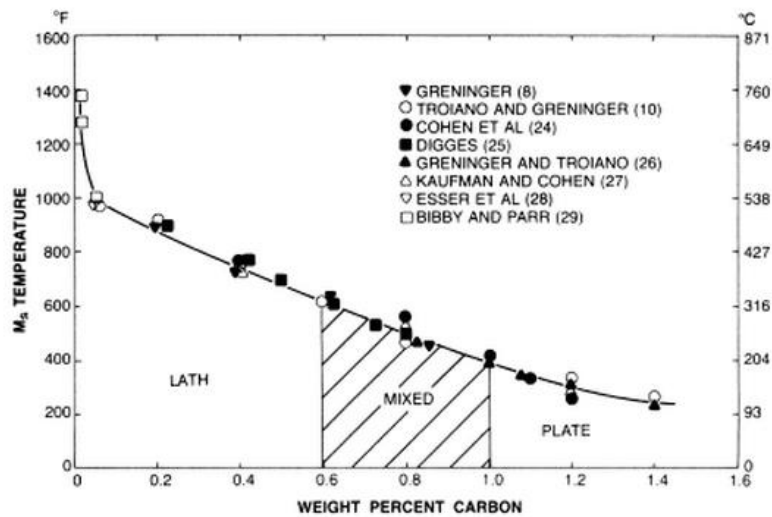


Figure 2. M_S -temperature plotted against the carbon content, as well as a description of the relationship between carbon content and the appearance of lath and plate martensite [7]

Lath martensite appears in packets. A packet consists of laths with the same habit plane but with different crystallographic orientations and can be seen as individual grains. The packets form a substructure inside the prior austenite grain, and are an important factor when it comes to mechanical properties. Inside each packet, laths with the same crystallographic orientation subdivide into blocks, as seen in Figure 3. Plate martensite does not appear in packets, which makes the formation of lath packets an important factor in low and middle range carbon steels. [6][8]

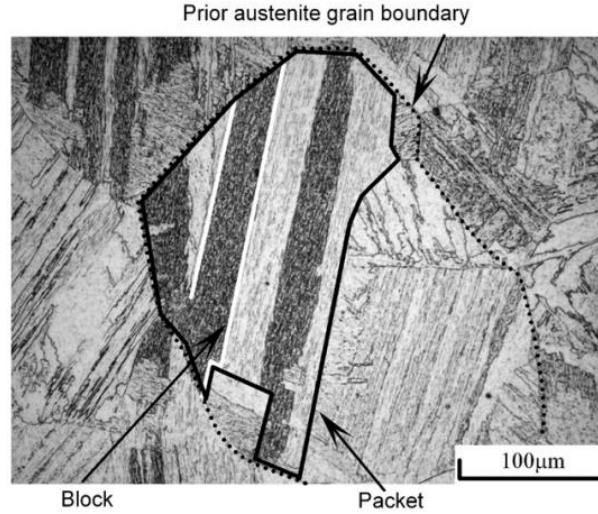


Figure 3. An illustrative image of the relationship between the prior austenite grain and the martensite packets and blocks [9]

The strength of lath martensite can be explained by the following equation

$$\sigma_y = \sigma_0 + \sigma_p + \sigma_s + \sigma_\rho + k_{HP}d^{-1/2} \quad (1)$$

σ_0 = friction stress for pure iron,

σ_p = precipitation hardening,

σ_s = solid solution hardening,

σ_ρ = dislocation hardening and

$k_{HP}d^{-1/2}$ = grain boundary strengthening, hall peatch

The strength related to the packet and the block size (d) is the Hall Petch term, and is valid for high-angle boundaries. High angle boundaries is boundaries with a high misorientation ($>15^\circ$). [10] Both packets and blocks form high-angle boundaries and will act as barriers for moving dislocations during plastic deformation. Smaller grains provide smaller packets which consequently give smaller blocks. According to the Hall Petch term, smaller units (grains, packets and laths) will increase the strength of the material. Smaller units results in more high-angle boundaries and thereby more obstacles for moving dislocations. [8]

Increase in grain size will increase size of the martensite plates consequently resulting in a higher risk for formation of microcracks. Moreover, longer and thinner martensite plates are more likely to form micro cracks causing a decrease in toughness and strength. Microcracks forms on the tip of the growing plate, when the strain is high enough to induce a crack. [11] Steels with high carbon content are more prone to microcracking, which involves formation of plate martensite. However, microcracking has also been seen in lath martensite. [7]

Prior austenite grain size will have a large impact on the strength of the final material. The formation of lath martensite in low and middle range carbon steels will help to subdivide the grains, resulting in more obstacles for moving dislocations during plastic deformation. Lower carbon content will lead to increased packet and block size. Finer austenite grains will consequently result in smaller packets and thinner blocks. [10]

However, it has been shown that formation of lower bainite needles upon cooling will help to subdivide the austenite grains further, and could therefore increase the strength even more, after subsequent martensitic formation. The interaction between martensite and lower bainite is interesting, and the two structures have shown to support each other.

2.2. Formation of Bainite

Depending on the cooling rate and alloy composition, austenite can transform into different phases and structures. The formation of martensite is related to rapid cooling, or diffusionless transformation, as discussed in Section 2.1. Martensite is a hard and brittle phase, but can be tempered to have a high toughness due to reduced residual stresses and a decrease in dislocation density.

Slower cooling rates often result in pearlite, a lamellar structure of ferrite and cementite, which is formed at relatively high temperatures. Ferrite and cementite grow side by side to form pearlite, by a so-called edge growth. Pearlite is a soft and ductile structure and is not desired in high pressure applications. However, at lower temperatures (550°C down to M_s), the mechanisms behind the formation of ferrite and cementite are different, resulting in a non-lamellar structure. The diffusion of carbon gets sluggish at lower temperatures, resulting in a fine and complex structure called bainite. During the transformation into bainite, ferrite is the leading growing phase, and the formation of cementite will occur when the carbon concentration, of the surrounding austenite or the ferrite phase, is high enough to allow precipitation of carbides.

The growth of bainite and the mechanisms behind it have been a topic of debate for a long time. Two main theories are generally discussed: diffusionless and diffusional theory. As the names reveal, the theories explain independent mechanisms that depend on diffusion or diffusionless transformation. [12]

2.2.1. Diffusionless growth

The diffusionless formation is described to be caused by a shear mechanism. Atoms are moving simultaneously in a glide-type motion which is called a displacive motion. [13] The diffusionless theory suggests that the transformation of bainite is a result of small subunits of ferrite that are formed similar to martensite. The austenite surrounding the ferrite will have an increase in carbon content and the formation of cementite will eventually take place. When the formation of cementite occurs, it will result in new sites for ferrite nucleation. [12] Moreover, studies have shown that no redistribution of substitutional atoms occur during formation of bainite. Therefore, it is possible to reject any growth mechanisms dependent on substitutional diffusion. [14]

The formation of bainite is associated with a surface relief, the same thing happens during martensite formation. Experiments where austenite grains have been polished in order to study the bainite formation have revealed that the surface is provided with a curvature after austenite transformation into bainite, also called plastic relaxation. This type of phenomena is often associated with displacive growth, and a similar phenomenon was discussed for martensite formation in section 2.1. [14]

The decomposition of austenite into bainite is divided into the following steps:

1. Nucleation of plates/subunits of bainitic ferrite on the austenite grain boundary.
2. The next nucleated subunit is nucleated on the tip of the previous formed subunit.
3. A number of subunits will eventually form a so-called sheaf.
4. Carbide formation on the ferrite/austenite interphase, or inside the ferrite plate

The precipitation of carbides influences the reaction rate by reducing the carbon content in the austenite or the supersaturated ferrite, as shown in Figure 4. The controlling growth mechanism is the growth of the sheaf, which is slower than the growth of a subunit. The formation of the later is considered martensitic. [15]

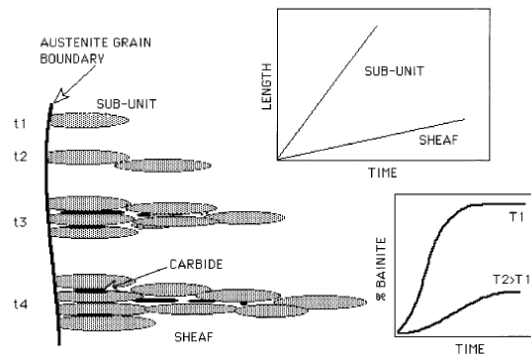


Figure 4. The nucleation of bainitic subunits takes place at the grain boundaries. Multiple subunits will eventually form a bainitic sheaf. [16]

2.2.2. Diffusional growth

The Diffusional theory describes the growth of bainite as a process controlled by redistribution of atoms, which involve diffusion of individual atoms away from the ferrite/austenite interface. [13] The diffusional theory also claims that the formation of bainite is initiated by formation of acicular ferrite or widmanstätten ferrite plates on the austenite grain boundaries parallel to each other. [15] In the temperature region between 550°C and M_s , the driving force for formation of ferrite is high. As the temperature decreases the equilibrium content of carbon in austenite will increase, this can be seen studying the Fe-C diagram, by following the equilibrium line for ferrite and eutectoid structure where the carbon content in ferrite decreases with temperature, resulting in a redistribution of carbon to the untransformed austenite. The result is a rapid transformation to ferrite. Between the ferrite plates a mix of ferrite and cementite is formed.

The difference between pearlite and bainite growth, according to the diffusional theory, can be seen in Figure 5. The redistribution of carbon is necessary in order to form ferrite and cementite. Lamellar pearlite is formed because the carbon atoms only need to move a short distance. Higher mobility will allow carbon atoms to move longer distances which results in thicker lamellas. However, the transformation into bainite is due to the limited diffusion rate of carbon due to the low temperature, resulting in a finer distribution of ferrite and cementite. [12]

Diffusion of carbon increases the carbon content in austenite, resulting in carbides. The diffusion allows low carbon ferrite to grow, and is affected by the equilibrium carbon concentration at the interface between ferrite and austenite. [14]

As discussed for the diffusionless theory the formation of bainitic ferrite is associated with a surface relief, and was brought up as evidence that the formation type is martensitic. However, in the diffusional theory the formation of acicular ferrite is assumed to be identical to the formation of widmanstätten ferrite. [12] Widmanstätten ferrite together with widmanstätten cementite is also formed with a surface relief. However, today the formation of widmanstätten ferrite and widmanstätten cementite is generally considered among researchers to be diffusional. [12]

Many scholars still consider the diffusionless theory, explaining that bainite is formed at temperatures below pearlite transformation. However, Hillert rejects the theory for diffusionless growth of martensite by assuming that the plate formation is the same as for acicular ferrite, and that the acicular transformation is the same as for widmanstätten ferrite. [14]

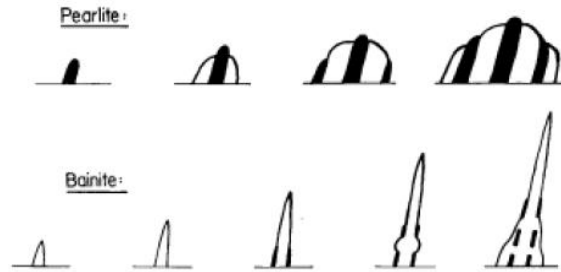


Figure 5. Difference in ferrite and cementite formation in pearlite and bainite can be separated by the distribution of the carbides and ferrite. Pearlite will have a lamellar structure, which is not the case for the bainite structure. [12]

2.3. Upper and lower bainite

Depending on the transformation temperature and the carbon content of the steel alloy, can result in different kinds of bainite. Two main types of bainite are going to be discussed, upper and lower bainite, which form at upper or lower temperatures. [12] The variation in morphologies between the two types of bainite is due to different rates of carbon rejection, which is the transportation of carbon away from the area, which will in a subsequent scenario transform into ferrite. The variation in morphology between upper and lower bainite is also due to the difference in growth mechanisms, and is related to the temperature at which the two structures are formed.

The coherency of the interface between ferrite and austenite during growth, will affect the bainite morphology, resulting in different ferrite appearance. Upper bainite have so called lath formed ferrite while lower bainite consists of ferrite with plate like appearance. Upper and lower bainite have low and high coherency respectively, resulting in a more rapid growth of the ferrite phase in lower bainite formation. [17]

The transition temperature, where upper bainite formation shift and lower bainite starts to form, is dependent on the carbon content, see Figure 6. The upper to lower bainite transition temperature is explained in the work of Ławrynowicz, and is defined as, “the highest temperature at which time required to obtain chosen volume fraction of cementite precipitation is smaller than the time necessary to decarburize ferrite lath”. [18]

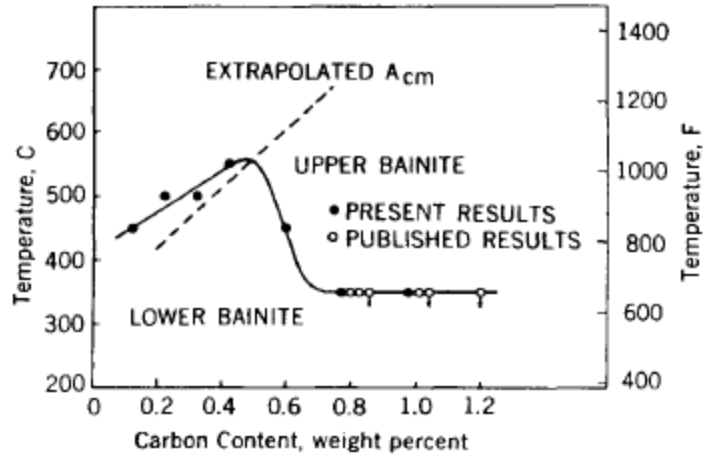


Figure 6. The relationship between the upper to lower bainite transition temperature depends on the carbon content.[19]

During the formation of upper bainite, the carbon mobility is high and carbides are formed on the interface between the austenite and ferrite lath. During the formation of lower bainite, the diffusion of carbon is limited and carbides are formed inside the ferrite phase, see Figure 7. [12] It has to be mentioned that the formed carbides do not have to be cementite; evidence of other types of carbides formed in lower bainite has been reported. [14]

The two different bainite structures have different ferrite morphology and carbide distribution, resulting in difference of the mechanical properties. [20] One explanation to the superior mechanical properties of lower bainite is that lower bainite have finer and more evenly distributed carbides, resulting in a higher necessary force in order for dislocations to pass carbides during plastic deformation. [21] [12]

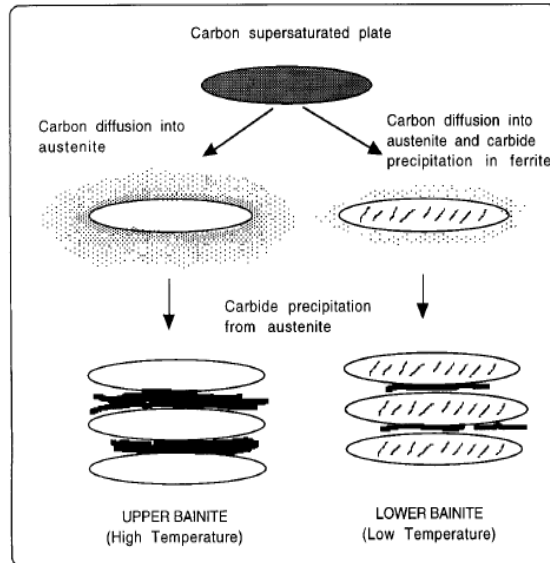


Figure 7. Schematic picture of the distributed carbides in upper and lower bainite. Lower bainite have carbides with in the ferrite subunits and between the ferrite plates. Upper bainite only have carbides precipitated between the ferrite plates. [12]

The typical appearance of bainite is small plates/laths of ferrite with similar orientation, adopted from the prior austenite grain, together forming a sheaf. [12] Lower bainite forms a needle-like structure with cementite precipitating on the austenite/ferrite interface as well as inside the ferrite plates. Upper bainite forms a more feathery-like structure with cementite only nucleating on the austenite/ferrite interface. Instead of plates, the upper bainitic ferrite forms long laths. [12] From the work of Tomita and Okabayashi, Figure 8 shows the difference in appearance of lower and upper bainite in a matrix of martensite. [1]

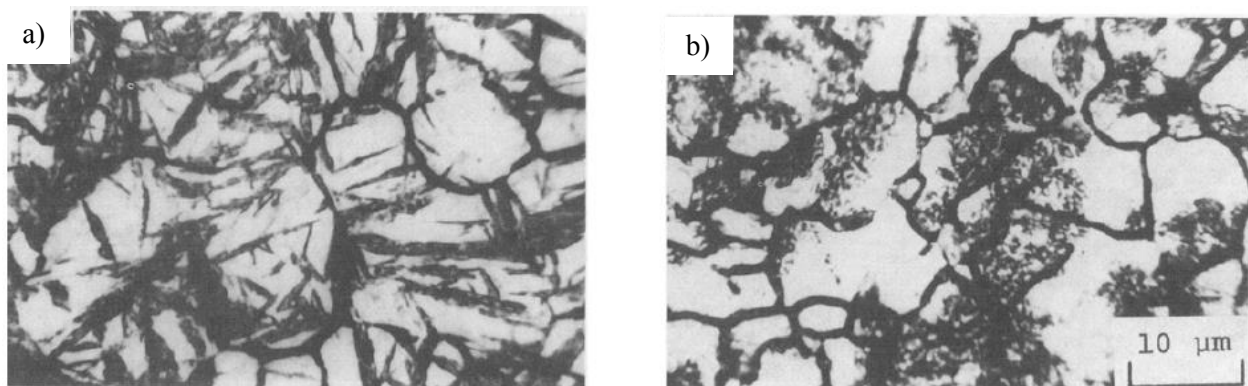


Figure 8. Not only the carbide distribution distingusih the upper and lower bainite strucutres from each other. The feerite morphology is also different for the two strucutres. Lower bainite have a needle like apperance and the upper bainite have a more feathery like strucutre. a) Lower bainite in a matrix of martensite. b) Upper banite in a matrix of martensite [1]

2.4. Combination of Martensite and Bainite

In alloys such as AISI 4140 and 4340, it has been shown that a mixture of lower bainite and martensite is preferred in order to enhance the mechanical properties.

One important parameter influencing the strength of the material is the prior austenite grain size. It has a big influence on the final properties. Smaller grains will increase strength since the size of the martensitic lath packets and blocks is directly related to the size of the austenite grains. [6][8]

Moreover, research has indicated that the size, shape, distribution and type of bainitic structure will have a big impact on the martensite strength. For example, when the acicular bainite is formed, it will subdivide regions of austenite and has a refining effect on the austenite grain size, resulting in smaller units.

Different research reports that lower bainite in ultrahigh tensile strength steel and in the presence of martensite will grow from the grain boundaries and take an acicular form. This particular structure will aid the material when it comes to toughness and strength. [8] [1] How large the refinement is of the martensitic structure, depends on the width (W_{LB}) and length (L_{LB}) of the bainitic sheaf, which will affect the martensitic size (S_{UM}). [21]

The bainitic structure forms before martensite and is therefore a controlling factor for martensite transformation, or the distribution of martensitic phases. Finer austenite grains and acicular bainite will together have a refining effect on the martensite packet size. Moreover, the strength of the bainite structure will increase due to the surrounding martensite. The martensitic phase will protect the bainite structure and limit its deformation, resulting in an increase in total strength of the material. [2] [16] For example, ultrafine duplex microstructures have been shown to be beneficial due to the secondary ductile phase (bainite) being alternated with a harder phase (martensite), resulting in an increase in mechanical properties. [1]

It has also been found that there is a large difference in mechanical properties depending on which type of bainite that is formed. Lower bainite has higher strength and ductility than upper bainite, and when combined with martensite, the difference is even larger. [20]

The presence of upper bainite has impairing effects on the properties due to the morphology. Instead of dividing the prior austenite grain into smaller subunits, like the lower bainite needles does, the upper bainite structure fills up the prior austenite grain, which restricts the refinement of the martensite structure, as seen in Figure 9. The decrease in strength of the mixed upper bainite/martensite structure is caused by a non-uniform strain that occurs during the initial stages of plastic deformation between upper bainite and martensite. The non-uniform strain occurs due to high local internal stresses caused by different deformation of the two structures and initiates close to the martensite/bainite interface. Upper bainite is deformed before martensite and will

therefore have an impairing effect the mechanical properties. The two structures do not support each other, unlike what occurs in lower bainite and martensite mixed microstructure. [20]

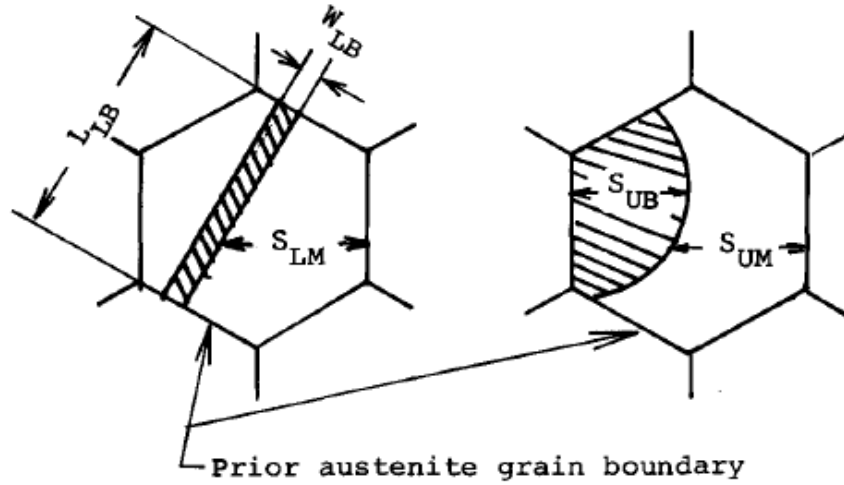


Figure 9. Schematic picture of the partitioning of the austenite grain caused by the upper and lower bainite structure. Lower bainite have a more refining effect on the austenite grain. Better refining can to some degree increase the strength of the martensite structure. [21]

The level of mixture and the quantity of each phase seems to influence the total strength of the steel a great deal, and can be related to the role of mixture. Equation 2 has been developed from the equation for role of mixture in order to describe the relationship between the strength and bainite content. The refinements of the martensite packets have been taken into consideration. [20]

$$\sigma_{0,2}^{mix} = (\sigma_{0,2}^M + kS_M^{-\frac{1}{2}})(1 - V_B) + \sigma_{0,2}^B V_B \quad (2)$$

$$\sigma_{0,2}^{mix} = \text{Yield strength of mixed structure}$$

$$\sigma_{0,2}^M = \text{Yield strength of martensite}$$

$$\sigma_{0,2}^B = \text{Yield strength of bainite}$$

$$V_B = \text{Volume bainite}$$

$$S_M = \text{Martensite packet size}$$

$$k = \text{Constant}$$

The equation is relied upon two assumptions

- The average lath width and packet size, S_M , will decrease when the bainite level, V_B , increases. This results in a refinement of the substructure, and is responsible for the increase in strength related to the Hall Petch relation, see equation 3.

$$\sigma_{0,2}^M = \sigma_i + kS_M^{-\frac{1}{2}} \quad (3)$$

$\sigma_i = \text{Friction stress}$

- The second assumption is that $\sigma_{0,2}$, for bainite, $\sigma_{0,2}^B$ in equation 1 is approximated to be fully bainitic steel. [20]

Lower bainite contents up to 25%, will result in substantial improvements of the mechanical properties, and caused by the high deformation strain of the bainite structure. The $\sigma_{0,2}^B$ reaches that of $\sigma_{0,2}^M$ and will result in a new expression for $\sigma_{0,2}^{mix}$, see equation 4.

$$\sigma_{0,2}^{mix} = \sigma_i + kS_M^{-1/2} \quad (4)$$

Equation 4 is valid up 25% lower bainite. Above 25%, equation 2 correlates well with experimental data. [20]

It has been demonstrated that the ferrite plates in the bainite structure can change a cracks path during its advancement in the material, thereby delay or even prevent cracks from propagating. [4] This phenomenon, together with an increase in strength, has shown to be valid only at lower levels of bainite, and its contribution will decrease at higher bainite content, see Figure 10. [22] Studies also show that for a given prior austenite grain size, the martensite packet size will decrease with higher levels of bainite. [2]

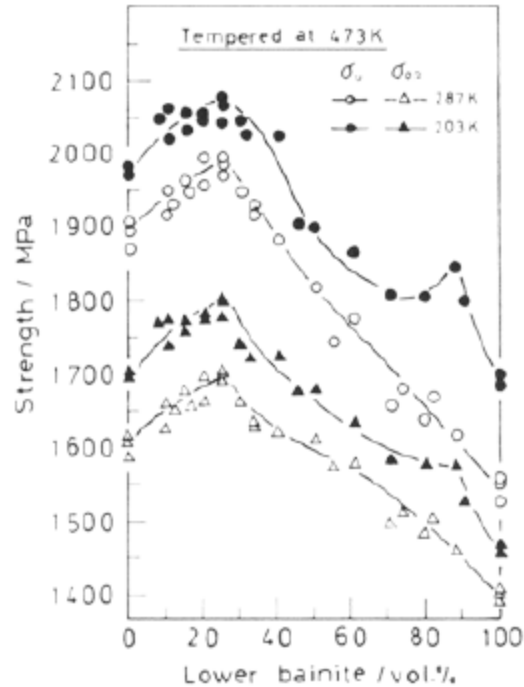


Figure 10. AISI 4140 steel, strength as a function of lower bainite content. There is a peak in strength at 25% lower bainite. [1]

Even though grain size is not a varying parameter in this study, it is important to have it in mind, in order to understand the transformation process and the resulting microstructure and the influences it will have on the final material. In order to control the microstructure, grain size etc., it is necessary to understand the heat treatment influencing the transformation of austenite, which is determined by carbon and alloy content, cooling rate and stresses in the material. [23]

The prior austenite grain size do not only influence the martensitic packet/blocklet size and bainite sheaf size, it will also affect the transformation kinetics of bainite during its formation. Lambers *et.al* studied the effect of austenitization before transformation into bainite. They concluded that that the larger austenite grains will increase the incubation time for bainite formation. [24] They also concluded that the presence of residual carbides after austenitization would lower the incubation time, due to more nucleation sites. [24]

Bhadeshia claims in his report on the bainite structure, that the difference between upper and lower bainite is the carbide distribution. [15] The formation and appearance of the lower bainite structure can vary, depending on temperature. The hardness of the bainite structure depends on the distribution of carbides, which also helps to distinguish between upper and lower bainite. [15]

Ohtani et.al claims that different types of upper bainite can form in low carbon steels. Depending on the temperature the carbide distribution together with the morphology of the upper bainite sheaf will vary. They say that three different kinds of upper bainite exist. The difference between the types is the distribution and the shape of the carbides, and the morphology of the ferrite phase. One specific type called upper bainite III is described as having cementite particles within the ferrite plate, resulting in better strength. They say that it is reasonable to classify this structure as a type of upper bainite because it has typical upper bainite ferrite morphology, in form of laths. The work of Ohtani et.al further illustrates the disagreement among researchers about the definition and complexity of the bainite structure. [25]

During continuous cooling, the formation of needles and sheaves that are associated with bainitic structure is dependent on the temperature during cooling. During the formation of the lower bainite structure, the carbide distribution and morphology of the bainitic ferrite are also dependent on temperature. [1][15] Quenching to lower temperatures is associated with a high driving force for transformation, but the lower temperature restricts the carbon diffusion. Lower carbon diffusion and high driving force for ferrite formation will lead to the formation of the lower bainitic structure and the formation of long needles. The carbon atoms do not have enough mobility to diffuse across longer distances and therefore carbides are formed inside the ferrite subunits, creating the backbone of the lower bainitic sheaf /needle. [3]

Higher driving forces lead to more nucleation sites; together with the low diffusion and smaller grains the number of nucleation sites will increase. At low temperatures the growth of the lower bainitic needle and the amount of formed needles will lead to increased refinement of the austenite grain. The strengthening of the bainitic structure is due to the fact that the stronger surrounding martensite will restrict the deformation, enhancing the strength. After a certain amount of grain refining and up to 25% lower bainite, the strengthening mechanism will no longer have an increasing factor due to lower bainite having to carry the majority of the load. [1]

In order to get thin bainitic needles the transformation temperature seems to be the controlling factor. Longer time isothermally heat treated does not seem to result in thicker bainite needles. The parameter that most of all seems to control the thickness is the transformation temperature, lower temperatures leads to thinner bainitic needles. [18]

The primary reason for the high strength of the martensite-bainite duplex structure is the morphology of the lower bainitic needles which form during isothermal heat treatment at low temperatures close to the M_s . [1] Enhanced mechanical properties due to formation of lower bainite has only been observed, when lower bainite is formed by isothermal heat treating. Lower bainite formed during continuous cooling only have impairing effect on the properties, when combined with martensite. [26]

There is a variation ways to create bainite with different quenching mediums. [27][28] However, in order to form isothermally transformed bainite, isothermal heat treatment in molten salt is a well-established method. [2]

It can be difficult to distinguish the martensite and the bainite structures from each other. When it comes to distinguishing tempered martensite and lower bainite, G.R. Speich *et.al* says in their report on tempered steel that martensite will get a body central tetragonal lattice arrangement when the carbon level is more than 0.2 %. Under the 0.2% carbon limit it will have a BCC-lattice. [46] The BCT-lattice is a consequence of trapped carbon atoms. When trapped C atoms are allowed to diffuse and precipitate and form carbides, it could possibly lead to that the martensite BCT lattice will transform and have more uniform lattice parameters similar to BCC.

The lower bainite structure consists of ferrite (BCC) with fine dispersed carbides precipitated inside and between the ferrite plates. This also applies to the tempered martensite structure. However, one difference of the two structures is how the carbides are orientated inside the ferrite or tempered martensite phase. The intralath precipitated carbides in lower bainite have an orientation of 55-65 deg to the long axis of the bainite plates. The tempered martensite has carbides with multiple habit orientations, while lower bainite have carbides with a single habit orientation. This distinction can only be seen when studying the microstructure in a SEM or TEM [47].

2.5. Banded structures

Banding has been a problem in AISI 4140 steel and can have negative effects on the mechanical properties resulting in microcracks between areas with different harnesses.

Banding is a phenomenon in steel materials where fiber lines can be seen in the microstructure. Dark and light colored fiber lines are formed during etching due to variation in austenite transformation products in different bands.

The main cause of banding is inter-dendritic segregation during casting, and results in bands with different chemical compositions, which consequently results in bands with different austenite transformation products. Even though the chemical composition varies, it does not necessary lead to banding. If the cooling rate is rapid enough the whole sample will transform into martensite, which will provide a homogenous microstructure. But, the segregation can result in different martensite band with a variation in etching color due to the variation in chemical composition.

Different elements are more prone to segregation. Solute elements with high redistribution factor/partition ratio (k) will have higher tendency to segregate. One other important factor,

which will influence the redistribution, is the amount of the segregated element. For example, phosphorus (P) has a high k value but is often present in low amounts, because it is removed by a refining step during secondary steel making, due to the impairing effects it has on the mechanical properties. Manganese (Mn) on the other hand has a relatively low k , but is often added in higher concentrations, and will therefore have a bigger impact on the segregation. Certain elements will also influence other elements redistribution. Mn together with chromium (Cr) is strong carbide formers, and will affect the redistribution of C, by lowering the activity of C. Regions with high Mn and Cr content will therefore attract C, in order to increase the local C concentration. Elements such as nickel (Ni), Silicon (Si) and P will have an opposite effect on the C activity, and will reject C from areas with high concentrations of these elements. [6] The affinity between C and Mn, Cr, will make it very difficult to homogenize the material via normalization after forging. Even if the high temperature will lead to high carbon diffusion the diffusion of Cr and Mn is slow, and will attract the C, resulting in very little or no homogenization. Homogenization at a high temperature during a long time is necessary to reduce the inhomogeneous composition, see Figure 11, which shows how the distribution of Mn depending on homogenization temperature and time. The same relationship can be assumed to be relevant for Cr and other strong carbide formers. [41]

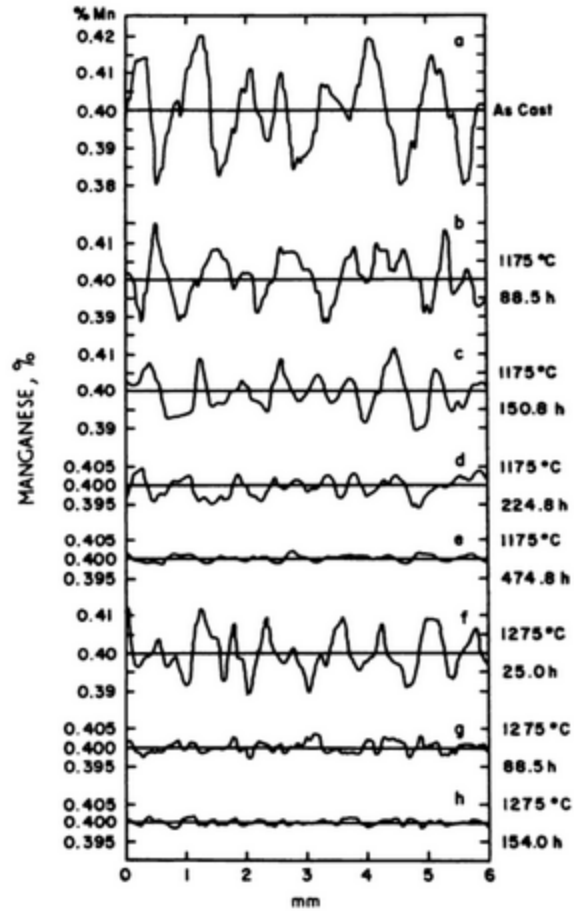


Figure 11. . The variation in strong carbon binder concentration after homogenization depends on the homogenization time and temperature. In this picture the Mn concentration is plotted against time and temperature. [42]

In the work of Garcia Navas *et.al* the authors claim that more fiber lines indicate a higher material flux which is a result of higher plastic strain. [41] The banded structures indicate inhomogeneity, and difference in deformation of the bar stock, and regions with higher density of bands is a result of higher more severe deformation.

2.6. Heat treating

The process of creating a martensitic structure is done by rapid quenching, fast enough to avoid the C-curves in the TTT diagram, see Figure 12. The C-curves represent diffusional transformation of austenite into pearlite and bainite. The area between y-axis, representing temperature, and the tip of the C curve is the shortest amount of time needed for austenite to transform into either pearlite or bainite, and is called the incubation time. Transformation will be fastest when the diffusion and the driving force for formation are both high. High incubation time will aid transformation to martensite, and can be increased by higher alloy content. Forming martensite through a fast quench is often performed on steels with more than 0.3 % C due to the fact that the increase in hardness is more significant for steel grades with carbon content equal to or higher than 0.3wt%. [6]

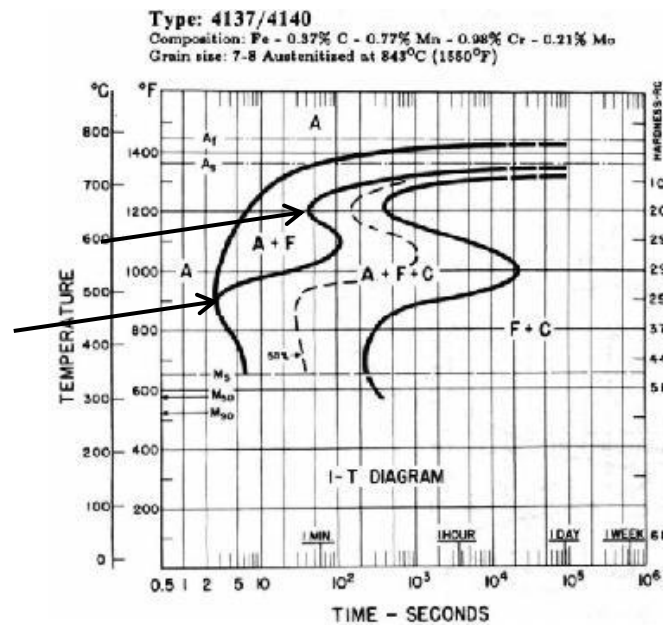


Figure 12.Is a picture of isothermal heat treating diagram of AISI 4140. The C-curves represent at which temperatures the diffusion controlled transformation of austenite is most rapid. Arrows point out the C-curves. [29]

At Cummins Fuel Systems, the products used in the fuel injection systems are quenched in order to form a martensitic structure. This has been a way to ensure certain properties including high hardness and toughness. The higher carbon content in austenite before transformation into martensite has an increasing effect on the hardness. There is an increase in dislocation density and a higher distortion of the BCC lattice, due to more trapped carbon atoms. The high hardness will consequently result in lower toughness and strength. Low toughness is mediated by a process called tempering, where the carbon atoms are allowed to form carbides and the

dislocation density is reduced. [23] However, research has shown that bainitic structures can have as good as or even better properties than tempered martensite. [22] Research reports that bainite is formed through quenching with different mediums such as gas, water or isothermal treatment in molten salt. [30][31] A variation of quenching speeds and mediums will be tested to better understand the formation of a mixed structure of bainite and martensite.

In order to design a heat treating process that produces a mixed microstructure, there are a variety of parameters that will have an effect, and needs to be taken in to consideration. The alloy content is one important factor, increasing the time austenite can be under the eutectic temperature without transform into other structures, resulting in a slower transformation. The foreign alloy atoms are occupying iron lattice sites, highly influencing the carbon mobility. Moreover, lower carbon mobility provides a better hardness profile, with a more even distributed hardness. [23] In order to control the final microstructure it is necessary to control the cooling rate. If the cooling rate is slow, the risk that austenite will be transformed into ferrite and pearlite is high. Faster cooling rates will suppress the diffusion of carbon, allowing austenite to transform into bainite and/or martensite. [23]

2.6.1. Quenching

During the quenching process the transportation of heat from the steel component is the deciding factor. The rate of the transformation of heat from the steel part will decide the amount and type of transformation products and consequently final microstructure. The heat transport can be divided into two different phenomena: conduction and convection. Conduction is the transport of heat from the interior of the sample to the surface and convection is the transport of heat away from the surface by the quenching media.

The quenching process can be divided into three different steps:

- A layer of vapor/steam is created close to the steel surface. The steam layer insulates the surface resulting in a low initial cooling rate.
- The vapor layer is broken down and the fluid will come into contact with the surface. The water then evaporates and forms bubbles, which are transported away from the surface. The cooling rate is rapid during this stage.
- When the surface temperature drops to a temperature below the boiling point of the fluid, the cooling rate is determined by the transportation of heat through either conduction or convection, resulting in a low cooling rate. [30]

The different steps are illustrated in Figure 13.

Parameters that influence quenching are: The circulation of the quenching medium, carbon and alloy content, austenite grain size and component thickness. [30]The agitation level will highly affect the three quenching steps and how long they are present. [23]

Research has shown that interrupted quenching can greatly impact the final product when it comes to phase transformation, distortion and residual stresses. Interrupted quenching makes it possible to manipulate the diffusion of carbon. Which enables the opportunity to control the cooling curve, and thereby the amount of different austenite transformation products. Isothermal heat treatment allows carbon diffusion to be somewhat controlled, thereby lowering the stresses in the material and resulting in fewer process steps such as tempering.

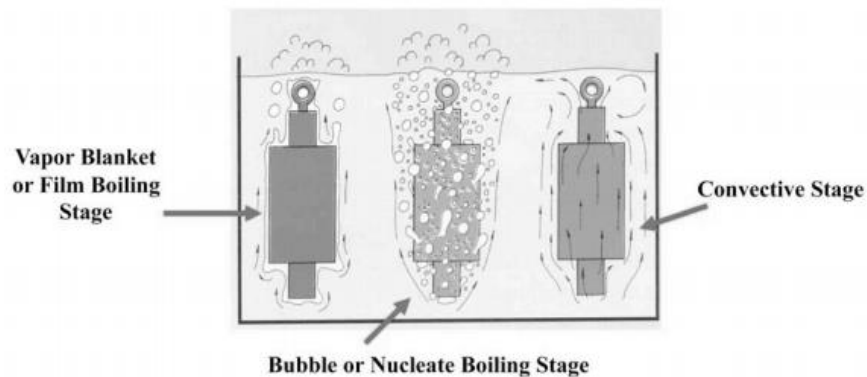


Figure 13. Different quenching stages in liquid quenching. A vapor blanket will be formed around the quenched part initially. When the temperature decreases bubbles will be formed on the surface and transported away from the surface. When the temperature has decreases further the transport of heat from the part will be controlled by convection. [30]

2.6.2. Oil quenching

Oil is commonly used as a quenching medium in order to get even and consistent mechanical and metallurgical properties. Oil quenching controls the heat transfer during rapid cooling and increases the wetting of the steel surface, limiting any thermal and transformational gradients which can cause distortion and cracking. Oil quenching is also beneficial because it is possible to predict the distortion pattern due to somewhat consistent heat transfer with similar geometries [30]

2.6.3. Gas quenching

During gas quenching, inert gas is blown over the steel surface. Heat is absorbed by the gas and is transported to water cooling heat exchangers, and then recycled back to the system for reuse. The process can be varied by controlling the temperature, velocity and pressure of the gas. Also,

the type of gas that is used will have a large impact on the transportation of heat from the quenched part. Inert gases are commonly used because no chemical reactions with the surface take place, and therefore post-heat treatment surface finishing is not necessary. Typical gases used in quenching are Argon, Helium, Nitrogen and Hydrogen. [23]

Gas quenching is able to achieve higher cooling rates compared to cooling in still air. Even though quenching with gas is slower than with oil, gas is used to reduce the risk of high distortion and cracking. Gas provides a more uniform hardness and is cleaner compared to liquid quench mediums. [23] Gas is often used for components with large sections, when a more uniform hardness profile is necessary. Components with thinner cross sections can be oil quenched because the boiling stage decreases with thickness, and the temperature where boiling takes place increases as the geometry decreases, and can provide a relatively even hardness

2.6.4. Molten salt quenching

Quenching in molten salt is a popular way of attaining martensite, it allows for a more controlled cooling process, compared to conventional quenching methods e.g. in water, oil and gas. Quenching in molten salt is particularly applicable for steels with high hardenability. The risks of distortion, non-uniform hardness, thermal stresses and transformation stresses are decreased when quenching in molten salt.

Austempering is a cooling process where the steel is cooled rapidly in molten salt in order to prevent pearlite transformation. It allows isothermal heating at a low enough temperature to allow decomposition of austenite into bainite, due to the fact that molten salt can sustain higher temperatures without degrading compared to most quench oils [31] [32]. Quenching and isothermal heat treatment in molten salt enables isothermal heat treatment between the pearlite-C curve and the M_S temperature. Another benefit of quenching in molten salt is that the vapor layer does not form and therefore results in more rapid cooling at higher temperatures. [32]

Three different features in the TTT-diagram are necessary in order for austempering or martempering to be feasible:

- A low enough M_S temperature to allow bainite formation
- High hardenability so the formation of pearlite can be prevented
- Reasonable transformation times to bainitic structure, not too long. [33]

Due to its negative impact on mechanical properties, it is important to ensure that no upper bainite is formed; therefore it is necessary to isothermally heat treat at a temperature close to the M_S -temperature. [31][32]

2.6.5. Isothermal heat treating temperature

This project is on isothermal heat treating closely located around the M_S -temperature. The idea is to try to form lower bainite, by performing isothermal heat treatment as close to the M_S -temperature as possible without going below it. This idea shaped the isothermal heat treating in the first trial, Trial A. However, there have been reports on lower bainite formation under M_S . The reason is said to be, that thermal stabilization of the austenite phase take place initially when the temperature reaches just below M_S , at a so called arrest temperature T_a . This phenomenon will interrupt the martensite formation. The thermal stabilization will allow lower bainite formation, and will appear as thin needles in the material. Earlier work have indicated that this could also lead to thinner lower bainite needles than formed above M_S , and could possible result in better refining of the martensite packets. [43] Also, the formation of lower bainite seems to be slower due to the lower transformation temperature, and could therefore be better controlled. [1]

In steels with low carbon content the M_S -temperature can be relatively high resulting in the possibility of redistribution of carbon atoms during quenching, before reaching room temperature. This phenomenon is referred to as autotempering or quenchtempering. Carbon atoms segregate further during quenching to high energy areas e.g. areas with fine dislocation structure or to packet/lath boundaries, resulting in precipitation of cementite particles. Moreover, low cooling rate under M_S could result in so called autotempering. If the M_S -Temperature is high autotempering is consequently more difficult to prevent. [6] Autotempering is purposely used in some processes to temper the martensite, and similar to austempering reduce the amount of distortions and stresses. This reduces the necessary production steps, because tempering after quenching is not needed.

One way to prevent autotempering can be to use a lower isothermal heat treating temperature.

2.7. AISI 4140

The AISI 4140, also referred to as Chrome-moly steel, have good strength to weight ratio. 4140 is considered strong and have relatively high hardenability. Fully hardened AISI 4140 steel can reach 60 HRC. High hardness is related to the carbon content; higher carbon content will result in higher hardness and consequently higher wear resistance. AISI 4140 is used in systems for pressurized tubes, such as fuel injection bodies. Such systems create high pressure, which pulses up and down over long periods of time. The 4140 is easy to case harden in order to protect against wear and erosion. Creating a thin case by nitriding can increase the fatigue strength with up to 30%. The material used in this work is provided by Ovako AB. The composition restrictions are presented in Table 1. [36][37]

AISI 4140 can experience different kinds of embrittlement during or after heat treating *e.g.* Blue, temper and martensitic embrittlement.

Blue embrittlement is associated with precipitation hardening. The steel will experience increase in strength and a decrease in ductility, resulting in a brittle material. The name blue embrittlement, is related to that it occurs between 230-370 C which is called the blue heat range.

Tempering embrittlement is caused by precipitates of trace elements such as Mn and Cr. Local depletion of alloy elements at prior austenite grains resulting in intergranular cracks, along the prior austenite grain boundaries.

Martensite embrittlement is a result of two main phenomena; segregation of impurities *e.g.* P, to the grain boundaries during austenizing and precipitation of cementite particles between the martensitic laths during tempering. [38]

The composition range of different elements for AISI 4140 from Ovako AB can be seen in Table 1.

Table 1. General composition range of AISI 4140 (wt%) at OVAKO AB

Element		C	Si	Mn	P	S	Cr	Ni	Mn
AISI 4140H (326)	min	0.38	0.2	0.8		0.005	0.8	0	0.15
	max	0.43	0.35	1	0.015	0.01	1	0.2	0.25

2.8. Etching

In order to study a materials microstructure it is necessary to etch the mounted samples. Different etch-methods and etch-chemicals will help the researcher to reveal different information about the configuration of the microstructure. To be able characterize the microstructure is an important work to understand materials mechanical properties, which is related to the materials grains size, defects and the variation of formed transformation products.

The most common way of etching is to use a so called attack etch method. Attack etching is basically controlled corrosion where the different features of the microstructure will etch faster than other parts. The microstructure together with the etching chemical can be seen as an electrochemical cell. Different structures and phases have different electrochemical potential. Features with higher electrochemical potential will easier be etched.

Pearlite for example consists of ferrite and cementite. Ferrite has a higher electrochemical potential than cementite. The ferrite will act as an anode and the cementite structure as a cathode, resulting in a deeper etch of the ferrite phase. The deeper etch of the ferrite phase will result in a darker appearance, due to the difference in the reflection of the incoming light, when the surface

is studied under a light optical microscope. The bainite structure also consists of ferrite and cementite, but with a non-lamellar and a finer distribution of the two structures. There are a number of ways to reveal the bainite structure but the one most recommended is picral because it attacks the ferrite carbide interface. Nital do not etch two phase structures as good as picral. Nital attacks the ferrite grain boundaries and is used to reveal ferrite grains and as-quenched, untempered martensite. [39]

One alternative way of etching is by using a tint etching chemical. A tint etchant will instead of removing material as the attack etch do, deposit a film on top of the surface. The most common tint etchants are sodium metabisulfite or potassium metabisulfite. In this study the sodium metabisulfite is going to be used. The sulfide ions in the etchant will act as reactants and will form a film on the surface. Tint etching is a good way of revealing martensite in a mixture of structures. [39]

A mixture of attack and tint etchant is a way to better reveal the microstructure. The attack etchant will remove the oxide layer that forms on the surface when exposed to air. It is necessary to remove the oxide film in order for the tint etchant to etch uniformly over the whole surface. The sodium metabisulfite will then deposit a layer of sulfide on the surface. [39]

2.9. Point Counting Method

In order to count the amount of different structures in the material, pictures of the microstructure is going to be taken at 500x magnification. A point counting method is adopted from the two dimensional systematic point count method described more in detail by Hilliard and Cahn. [40] A pre-decided grid is used and is superimposed on the picture of the microstructure. Each corner in the grid/lattice represents a point. The amount of points which ends up inside the analyzed features, divided by the total amount of points, provides number of the percentage of the analyzed phase/structure. A schematic picture can be seen in Figure 14.

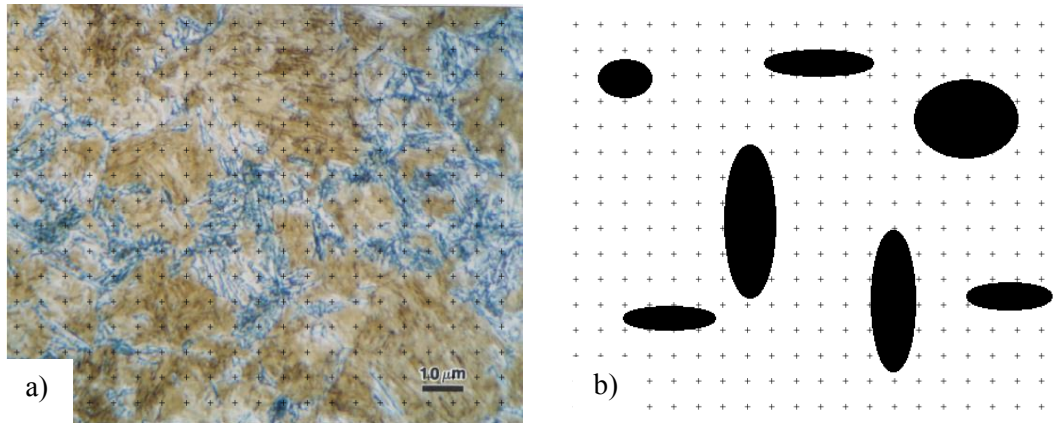


Figure 14. Schematic picture explaining the point counting method used in this study. The number of points within the features analysed divided by the total amount of point provide a percentage.

The grid of points should be coarse enough to ensure that not two adjacent point end up in the same feature. One other way of defining the necessary point space, is that the minimum distance between two adjacent points must be greater than any caliper radius of the studied features. [40]

3. Materials

The material is provided by Ovako AB and is AISI 4140 steels. Two materials, 326 F and 326 C, are going to be tested. The 326C is the standard 4140 steel from Ovako AB, while the 326 F is designed to have a higher hardenability. The difference in hardenability is due to the increased levels of Cr and Mo in 326F steel. Chemical composition for material 326F and 326C can be seen in Table 2 and Table 3 respectively.

Table 2. Chemical composition (wt%) Ovako steel grade 326F

C	Si	Mn	P	S	Cr	Ni	Mo	Cu	V	Al
0,42	0,25	0,94	0,011	0,006	1,05	0,12	0,23	0,126	0,008	0,027

Table 3. Chemical composition (wt%) Ovako steel grade 326C

C	Si	Mn	P	S	Cr	Ni	Mo	Cu	V	Al
0,42	0,24	0,95	0,009	0,009	0,99	0,14	0,17	0,15	0,009	0,027

The 326 F and C arrived as peeled bars and had been spheroidized annealed and hardened tempered respectively. Pictures of the microstructures can be seen in Figure 15.

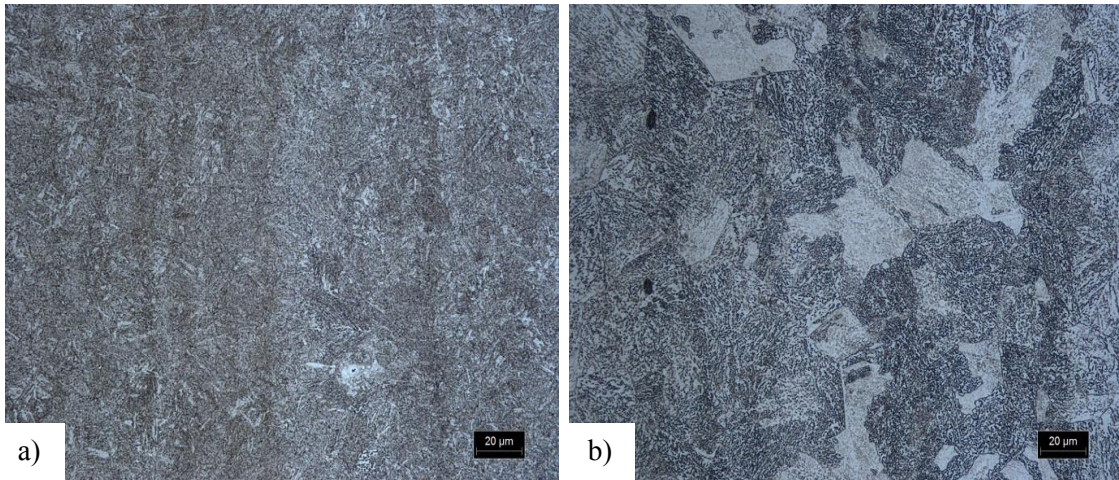


Figure 15. The microstructures of both materials were studied before heat treating. The two materials were heat treated differently at the supplier. a) Quenched and tempered 326 C x500, b) spheriodized annealed 326F x500. Both were etched with 2% nital.

The structure is finer in the 326C quenched and tempered material, while the 326F spheriodized annealed material has a coarser microstructure.

4. Experimental procedures

4.1. Sample preparation

The bar stock was cut into pieces of approximately 10 and 20 mm, see Figure 16. Three samples for each material, heat treatment and sample thicknesses were prepared. 326C and 326F have diameters of 36.5mm and 41mm respectively.

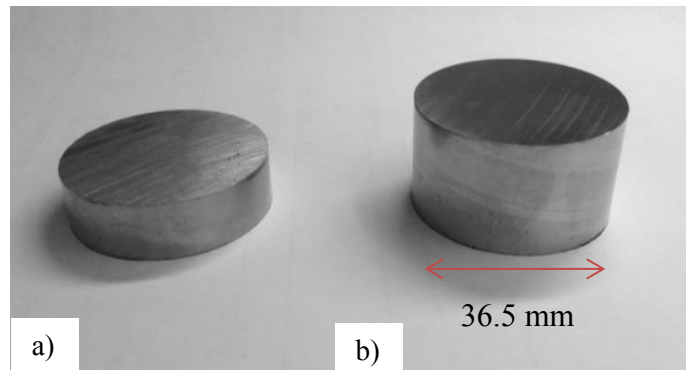


Figure 16. The bar stock were cut in samples with two different thicknesses, 10mm and 20mm. The picture shows the two different thicknesses of materila 326C with a diameter of

One other samples thickness is added to the heat treatment using the vacuum heat and gas quench method, the thickness is 45mm.

4.2. Sample analysis

In order to study the microstructural changes and hardness after heat treatment the samples where sectioned to investigate in the longitudinal direction, see Figure 17.

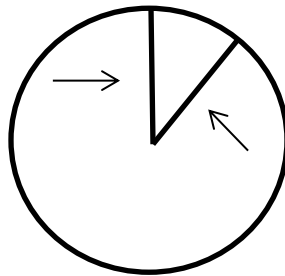


Figure 17. A Schematic picture showing the surfaces studied of each sample. The samples were investigated in the longitudinal direction of the bar stock.

Both micro and macro hardness tests were performed. Macro hardness test was taken on the surface of the samples, while the micro-hardness test was taken on the mounted surface of the samples. The microhardness readings were taken over the whole surface to see the hardness variation from the surface to the core of the sample. Five readings were taken on multiple locations on the surface, at the core and between the core and the surface, in order to study the homogeneity of the microstructure. An illustrative picture can be seen in Figure 18.

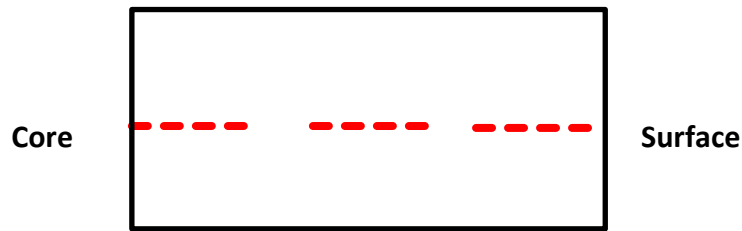


Figure 18. Schematic picture showing where the microhardness reading were taken. To better understand the variation in hardness between the surface and the core, readings were taken over the whole mounted surface.

The result was studied using well known statistical tools such as 2 sample T tests and one way anova tests, in order see any statistical differences between Trails, materials, sample thickness, radial hardness variation and time isothermally heat treated.

4.3. Heat treatment

Three heat treatments are going to be tested to study the bainite transformation in AISI 4140 steel. The heat treatments are further described in Table 4.

Table 4. Heat treatment performed in this work.

<i>Designation</i>	<i>Heat Treatment</i>
Vacuum heating and as quenching	Austenitizing at 843°C at 1.5 h in an atmosphere 100 micron vacuum, gas quenching (Nitrogen) at 2.758 barr down to room temperature.
Austempering, Trial A: (<i>Isothermal heat treating T=343°C</i>)	<ol style="list-style-type: none"> 1. Preparation step* 2. Austenitizing in molten salt at 871°C for 1h and placed in quench salt at 343°C for 60-120 s, then immersed in water for 1 min.
Austempering, Trial B: (<i>Isothermal heat treating T=320°C</i>)	<ol style="list-style-type: none"> 1. Preparation step * 2. Austenitizing in molten salt at 871°C F for 1h and placed in quench salt at 320°C for 60-120 s, then immersed in water for 5 min. 3. Tempered at 200°C for 2h

* *parts evenly spread out in basket and dried in 260°C for 15 min*

A schematic picture of the heat treatment cycle for Trial A and B can be seen in Figure 19. The difference between Trial A and B is the isothermally heat treating temperature, 343°C and 320°C respectively, and that a subsequent heat treating step is added to Trial B. The tempering step in Trial B is adopted to limit the risk for tempering embrittlement.

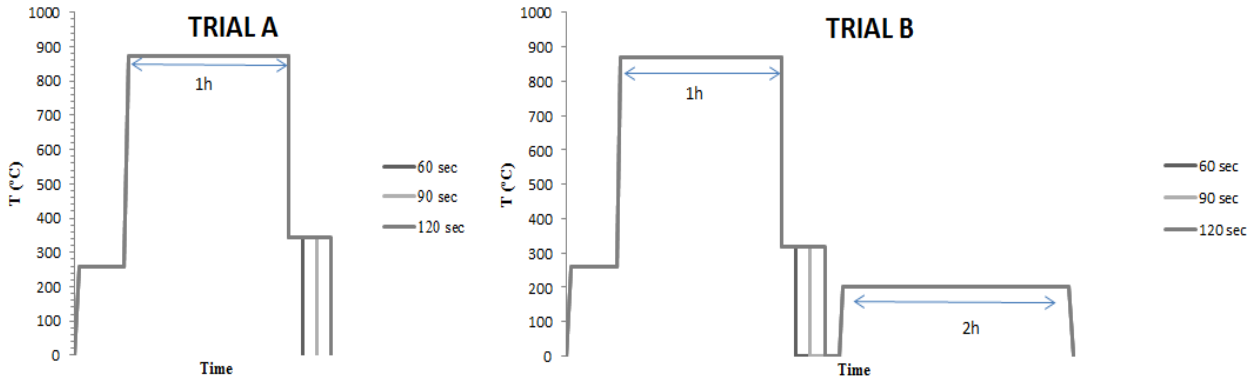


Figure 19. Schematic picture of the heating cycles. Trial A have a isothermal heat treating temperature higher than Trial B, and Trial B have a tempering step. The first step represents when the samples were dried before heat treating.

4.4. Etching methods

A variation of etching methods is going to be tested in order to study the variation of the appearance of the different structures when studied under a LOM. This is done in order to test and map the different etching opportunities and to do preparatory work in order to determine an etching process to better reveal, and distinguish as-quenched and tempered martensite from lower bainite. The chemicals used in this study can be seen in Table 5.

Table 5. Tested etching chemicals.

<i>Etchant</i>	<i>Description</i>
2% Nital	Attack etchant. One step process.
4%Picral + 5% Sodium metabisulfite in water	Attack etchant + tint etching. Mixed; the etching process consists of one step.
4%Picral+HCl	Attack etchant + surface agent. Mixed, the etching process consists of one step.
4% Nital + 5% Sodium metabisulfite in water	Attack etchant + tint etchant. Not mixed, two step etching process.

5. Result and Discussion

5.1. Vacuum heating gas quenching (VHGQ)

5.1.1. VHGQ test 1

Three samples with three different thicknesses were heat treated at 1550 F in vacuum (100 microns), and quenched in gas at 40 psi, in an atmosphere of nitrogen.

The banding is quite large, which indicates poorly or no homogenization after casting. Banding is caused by segregation, resulting in areas with difference in alloy concentrations, as seen in Figure 20.



Figure 20. Banded structure etched in 2% Nital.

In bands, with light colored structures, it is possible to see manganese-sulfur (MnS) particles, this proves that higher amount of Mn is present in these areas, as seen in Figure 21. MnS particles cannot be spotted in the darker bands. High amount of Mn would consequently lead to higher amount of C. The high Mn and C concentrations in these areas would therefore motivate the light colored structures as being martensite and lower bainite. Increasing Mn and C content pushes the C-curve in the TTT-diagram to the right, increasing the incubation time. Higher incubation time will support the martensite and lower bainite transformation. If the cooling is rapid enough and the sample is transformed into martensite, no band will occur, except for bands caused by the etching due to the different solute content the different martensite regions.

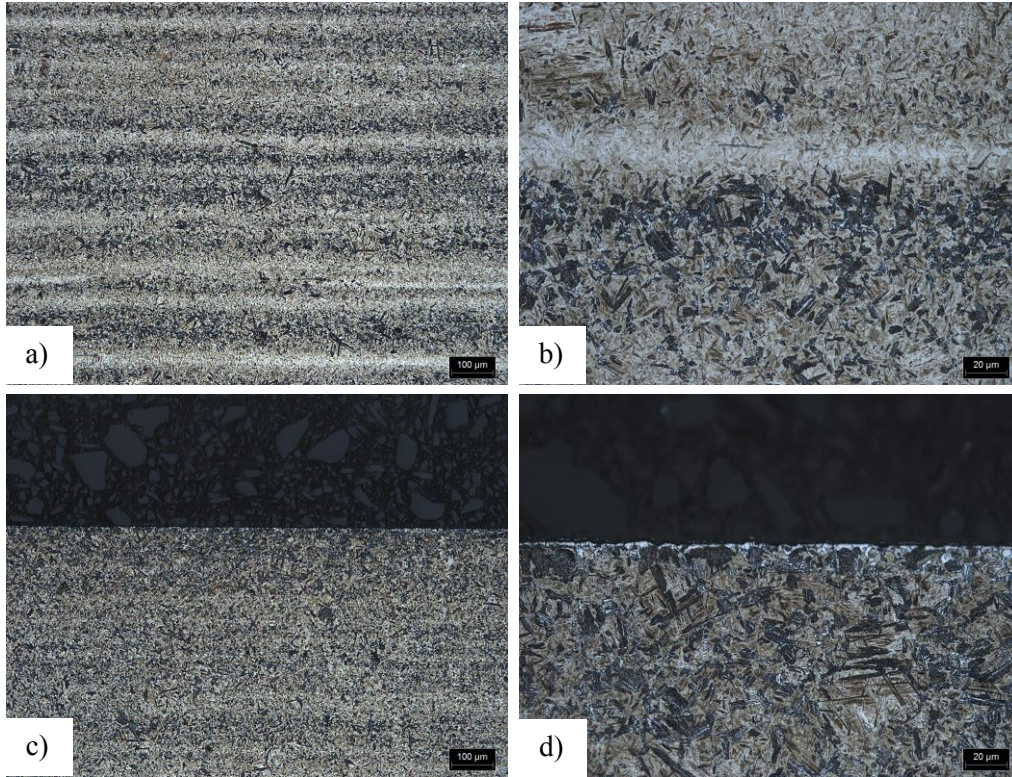


Figure 21. Pictures taken in LOM. a) Core with low magnification, b) core with high magnification, c) surface with low magnification and d) surface with high magnification

The macro hardness test revealed a higher hardness at the perimeter of the sample. The average macro-hardness is plotted against the samples thickness and can be seen in Figure 22. The decrease in hardness with increasing sample thickness indicates more non-martensitic transformation products in thicker samples.

Average hardness vs. sample thickness

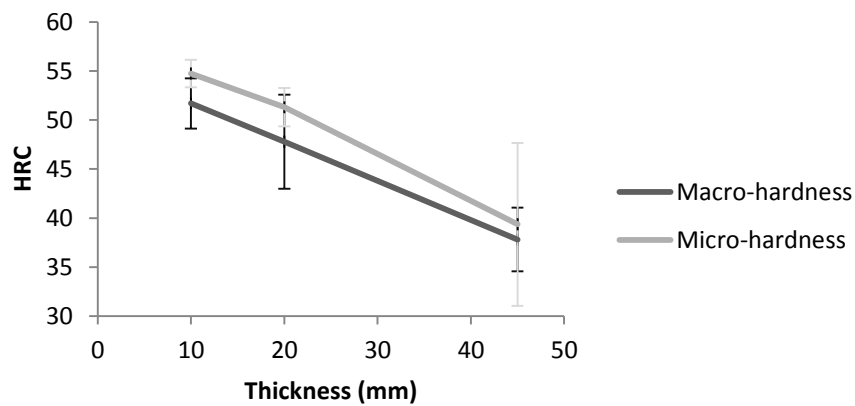


Figure 22. Average macrohardness and mirohardness plotted against sample thickness.

All three samples were quenched the same way in the same heat treating run. The variation in hardness between the three samples is almost linear. Samples with 10 and 20 mm thickness were both located around the 50-55 HRC specification range. But the variation between the highest and lowest value is >5 HRC, which is too much. The variation should not be higher than 5HRC because it could result in microcracks in the material. An example of such a region is the boundary between two bands. This is due to the variation in hardness between bands, resulting from the variation in chemical composition and consequently different hardenability.

It is possible to see some lower bainite structure in the images. But it is also possible to see ferrite and pearlite structures. Higher gas pressure initially during quenching can possibly reduce the amount of formed ferrite and pearlite, as-well as increase the agitation of the gas initially and then reduce the pressure and shut down the fan responsible for the agitation after a couple of seconds. This could possibly provide better result when it comes to reducing the ferrite and pearlite formation and support the lower bainite formation.

The formation of thin lower bainite needles seems to be necessary in order to result in a refinement of the martensite structure and thereby an increase in strength. The formation of needles is dependent on the temperature, low temperature is necessary. Moreover the needles need time to grow in order to partition the austenite grains. If this is possible by conventional gas quenching is not clear.

It should also be mentioned that an enhancement of the mechanical properties caused by lower bainite needles have not been seen in conventional quenching. Isothermal heat treating is necessary in order for this phenomenon to take place.

5.2. Austempering in molten salt

5.2.1. Trial A

Similar banded structure as seen in the vacuum heated and gas quenched samples can be seen in the samples isothermally heat treated in molten salt. The banding seems to be most severe in the center of the pieces, which indicates more segregation, and thereby a higher plastic strain in the center of the samples. In the work of Garcia Navas *et.al* the authors claim that more fiber lines indicate a higher material flux which is a result of higher plastic strain. [41] The banded structures indicate inhomogeneity, and difference in deformation of the bar stock, this is further discussed in section 2.5.

The purpose of the austempering in molten salt was to try to control the levels of formed bainite in a matrix of martensite. The banded structure makes it difficult to control the levels of bainite

and martensitic structures. The amount of formed ferrite and pearlite, if any, is also very difficult to predict, when the composition of the material is different depending on banded zones. High initial quenching rate is necessary in order to ensure that no pearlite and ferrite is formed.

Also, due to the segregation during solidification and the resulting banded structure. The variation of alloying elements in these bands could also affect the M_s -temperature for each band resulting in different amounts of bainite and martensite transformation products. This seems to be the case for most samples in Trial A. One way to test this could be to investigate the amount of retained austenite in each band.

The thinner samples showed a slightly higher surface hardness than the thicker samples, all materials and both thicknesses showed a peak in hardness after 90 s. Curves for each sample type are compared to each other in Figure 23. Material 326F has a higher surface hardness than material 326C. For the same thicknesses but different material, the average difference is around 1,4HRC. This probably a result caused by the higher Cr and Mo content in the 326F material resulting in a higher hardenability and thereby a higher surface hardness.

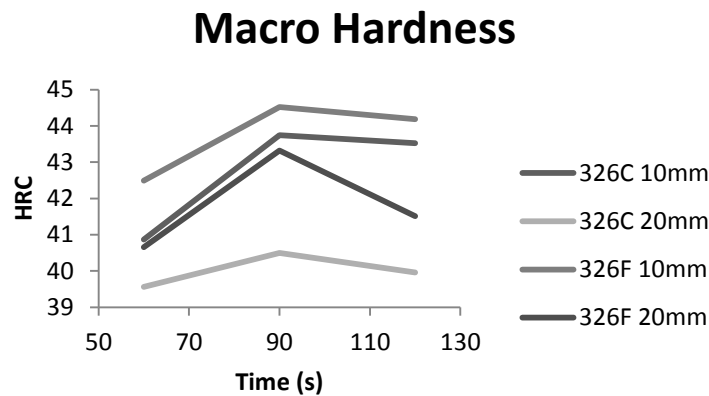


Figure 23. Hardness plotted against time in isothermal heat treatment. Different lines represent different material and thickness combinations.

Macrohardness result for each sample and time isothermally heat treated together with the standard deviation for Trial A can be seen in Table 6. The data is collected from all 36 samples, three readings from each sample.

Table 6. Macrohardness results from Trial A.

Sample	Macrohardness (HRC)		
	60s	90s	120s
326C 10mm	40.87 ± 1.73	43.74 ± 0.63	43.52 ± 0.60
326C 20mm	39.57 ± 0.62	40.5 ± 1.40	39.96 ± 2.38
326F 10mm	42.49 ± 1.17	44.52 ± 1.02	44.19 ± 0.57
326F 20mm	40.66 ± 0.29	43.32 ± 0.60	41.51 ± 1.15

The hardness restriction for this study is set to be within 50-55 HRC. A larger variation in hardness can lead to microcracks. A boxplot of each sample variation can be seen in Figure 24. Each box is an individual combination between: material (326C or 326F), samples thickness (10mm or 20mm) and time isothermally heat treated, (60, 90 or 120s). The dotted lines divide the graph into different time zones. The red reference lines show the 50-55 HRC restriction. Each box plot includes 15 data points.

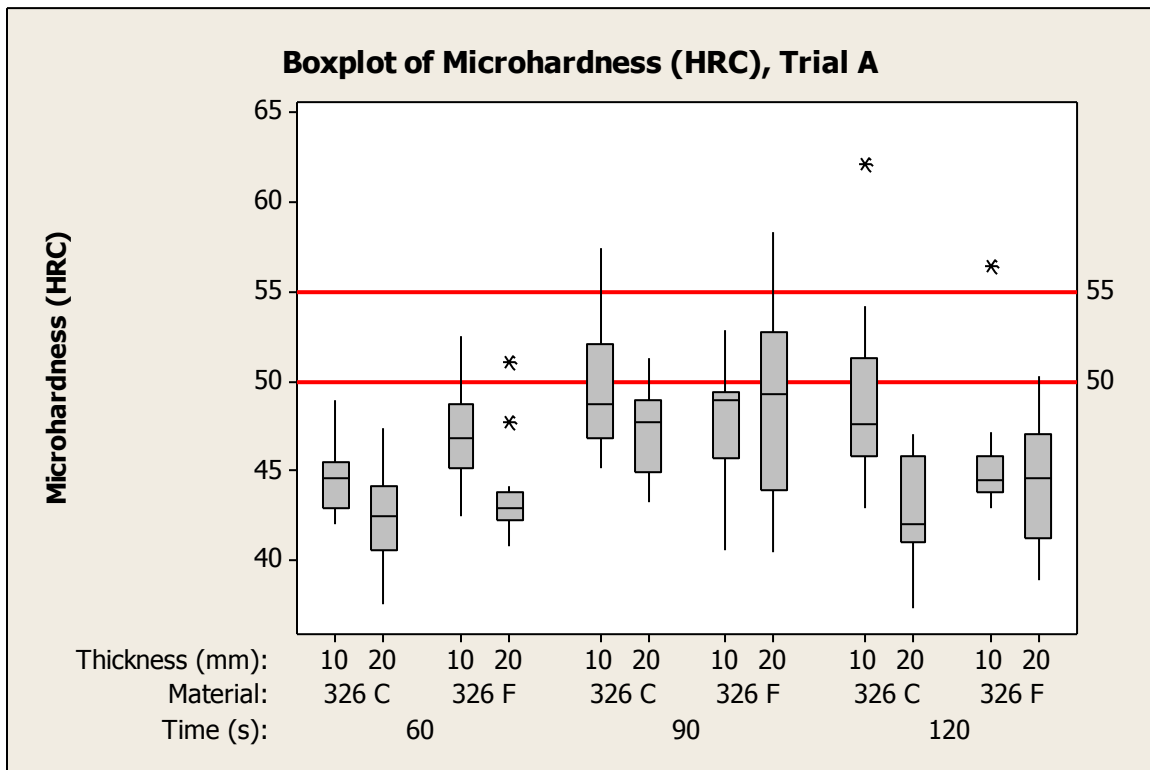


Figure 24. Boxplots of microhardness in Trial A.

The variation between the highest and lowest value is large and can be a result of the banded microstructure together with the expected surface to core variation, due to the relatively low

hardenability. The microhardness shows similar pattern as for macrohardness data except for the 326 F 10 mm, which have a lower hardness in relation to the other sample variations. More data have to be collected to further understand why sample 326F 10mm deviate. Average microhardness for each sample variation are plotted against isothermal heat treating time, see Figure 25.

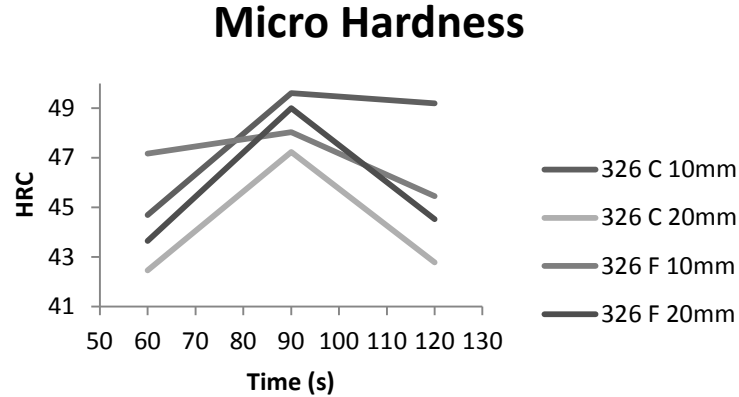


Figure 25. Microhardness plot for each sample variation and time isothermally heat treated at 650F.

Microhardness result for each sample and time isothermally heat treated, together with the standard deviation for Trial A can be seen in Table 7.

Table 7. Microhardness results from Trial A.

Sample	Microhardness (HRC)		
	60s	90s	120s
326C 10mm	44.69 ± 1.81	49.62 ± 3.80	49.2 ± 4.69
326C 20mm	42.46 ± 2.30	47.23 ± 2.48	42.79 ± 3.14
326F 10mm	47.17 ± 2.91	48.03 ± 3.34	45.45 ± 3.25
326F 20mm	43.65 ± 2.59	49.01 ± 4.92	44.52 ± 3.08

The 326 C seems to have some ferrite and pearlite in its microstructure after quenching. Ferrite and pearlite is not present in the same extent in the 326F material after heat treatment, see Figure 26. These pictures are representative for each material and thickness combination. Moreover, less non-martensitic transformation product is present in the 326F material, which is an indication that the higher hardenability, increase the incubation time, which makes it easier to create less amount of lower bainite structure. Moreover, less lower bainite content result in more

as-quenched martensite and consequently higher strength. All this is to be expected, due to the difference in alloying composition.

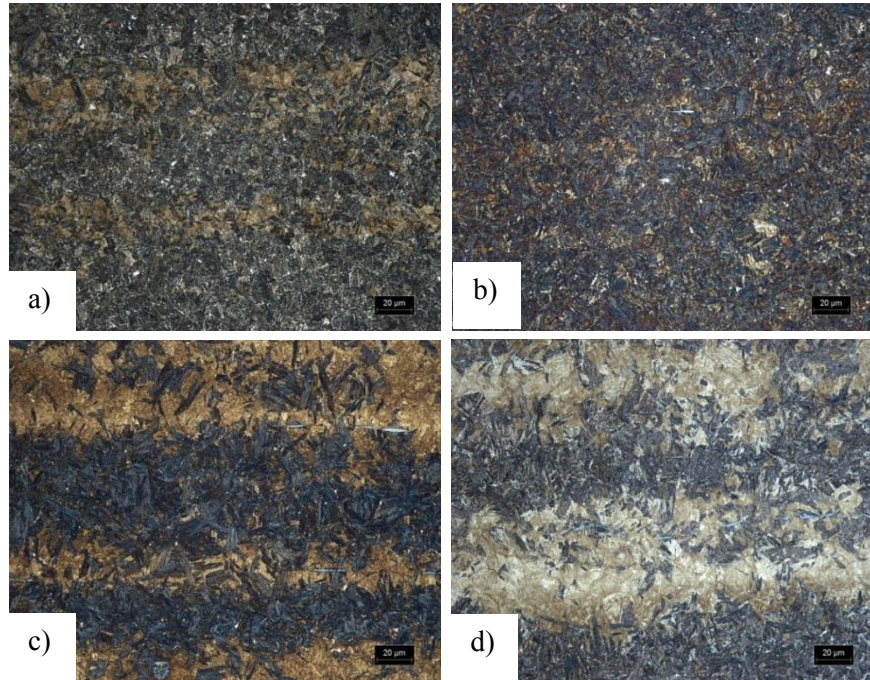


Figure 26. Representative images taken of the microstructures at x500 magnification after 60 s. a) 326 C 10mm b) 326 C 20mm, c) 326 F 10mm and d) 326 F 20mm

The microstructure before heat treating may have provided different circumstances resulting in variation in banding and amount of formed bainite. Material 326F had a more coarse microstructure before heat treating maybe it contributed to the less formed lower bainite in material 326F. The microstructure is finer for 326C than for 326F.

5.2.2. Isothermal heat treating temperature

The smallest amount of transformed bainite in Trial A was above 50%, lower isothermal heat treating temperature could possibly lead to less transformed lower bainite. Less lower bainite formation could provide better understanding of the refining effect that the lower bainite needles will have on the mechanical properties. The goal should be to reach the 25-30% lower bainite content that in earlier work have shown to enhance the strength of high-tensile steel. One way to reach this goal could be to lower the isothermal heat treating temperature.

Because of the presence of tempered martensite in the structure, it is likely that the cooling under M_s has not been fast allowing carbon to diffuse. Because no subsequent tempering process was performed in the Trial A the tempering of the produced martensite had to be tempered during the

quenching process. The isothermal heat treatment was conducted above M_S , which indicate that the cooling from isothermal heat treatment T down to room T was relatively slow.

It was decided to use an isothermal heat treating process under M_S and a subsequent tempering step, due to a variation of factors:

- It is difficult to distinguish the tempered martensite and the bainite structure from each other. In order to test etching methods to distinguish the tempered martensite and the bainite structure, it was decided to temper the samples in order to temper all martensite, and to see the difference between as-quenched and tempered martensite. The literature provides various methods to do reveal as-quenched martensite. But in order to better understand what separates the appearance of lower bainite and tempered martensite a tempering step was included in the heat treating plan for Trial B.
- One other reason to add a tempering step is to level out the hardness profile in the samples. It was shown in Trial A that the variation within the samples from the core to the surface was quite large. In order to ensure that no brittle as-quenched martensite was still present after heat treating, a subsequent heat treating step was introduced.
- In order to slow down the growth of the bainite structure, the isothermal heat treating was decided, in Trial B, to be performed under M_S . Hopfully resulting in less amounts of formed lower bainite.
- Lower isothermal heat treating temperature could possibly lead to an increase in quenching speed.

The tempering process is going to be performed on the boundary for temper embrittlement. AISI 4140 experience temper-embrittlement if tempered between 393 and 700 F.

Bainite formation under M_S has been studied before and the heat treating process was influenced by heat treating Trials designed by Tomita and Okabayashi [1]. The samples were isothermally heat treated at the same times used in Trial A, between 60 and 120 seconds, also adopted from the work from Tomita and Okabayashi. [1]

5.2.3. Trial B

A boxplot of the microhardness in Trial B can be seen in Figure 27. The microhardness is more evenly distributed between the core and the surface of the samples in Trial B compared to Trial A. Which indicates that the tempering process after isothermal heat treating had a positive effect on the hardness variation. The pattern seen in Trial A where the 326F material had a overall higher hardness than 326C is lost in Trial B, and can be a result of the subsequent tempering step. The average microhardness of each sample variation can be seen in Figure 28. When the samples were etched and studied under a microscope material 326F provided a better

microstructure when it comes to less or no pearlite and ferrite transformation products, which further indicates that the lower bainite and the tempered martensite have a similar hardness.

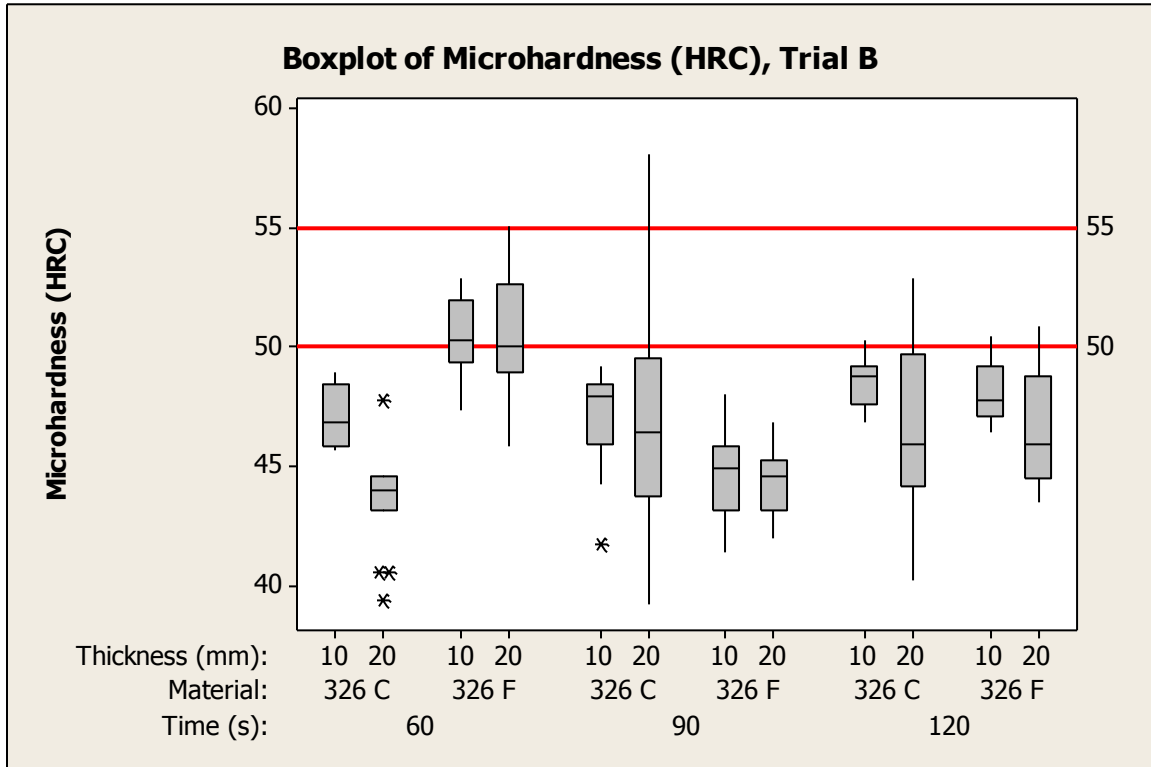


Figure 27. Box plot of the Microhardness for Trial B.

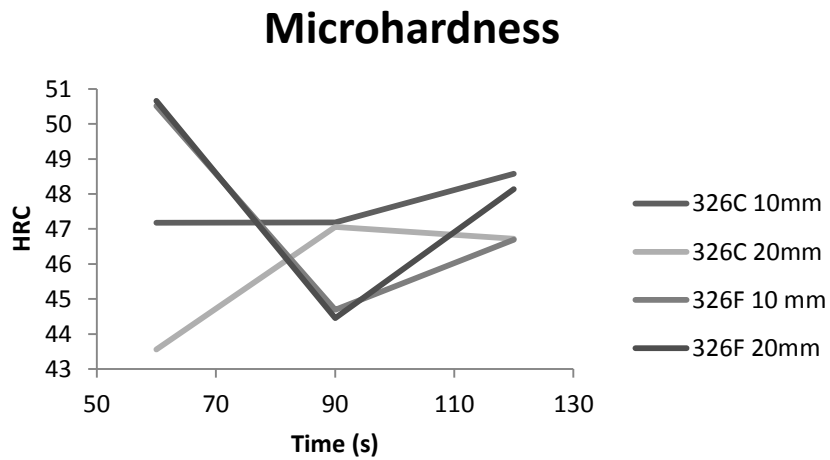


Figure 28. Microhardness plot for each sample variation and time isothermally heat treated at 608F.

Microhardness result for each sample and time isothermally heat treated, together with the standard deviation for Trial B can be seen in Table 8.

Table 8. Microhardness results from Trial B

Sample	Microhardness (HRC)		
	60s	90s	120s
326C 10mm	47.18 ± 1.26	47.19 ± 2	48.57 ± 1.08
326C 20mm	43.56 ± 2.04	47.06 ± 4.81	46.72 ± 3.55
326F 10mm	50.51 ± 1.50	44.70 ± 1.86	46.70 ± 1.21
326F 20mm	50.66 ± 2.42	44.45 ± 1.31	48.14 ± 2.19

Representative pictures for each material and thickness combination can be seen in Figure 29. The amount of non-martensitic transformation products is lower in the 326F than in the 326C material. It is reasonable to relate less amount lower bainite formed in material 326F to the higher hardenability. The typical needle like appearance of the lower bainite can be seen in Figure 29 c) and d).

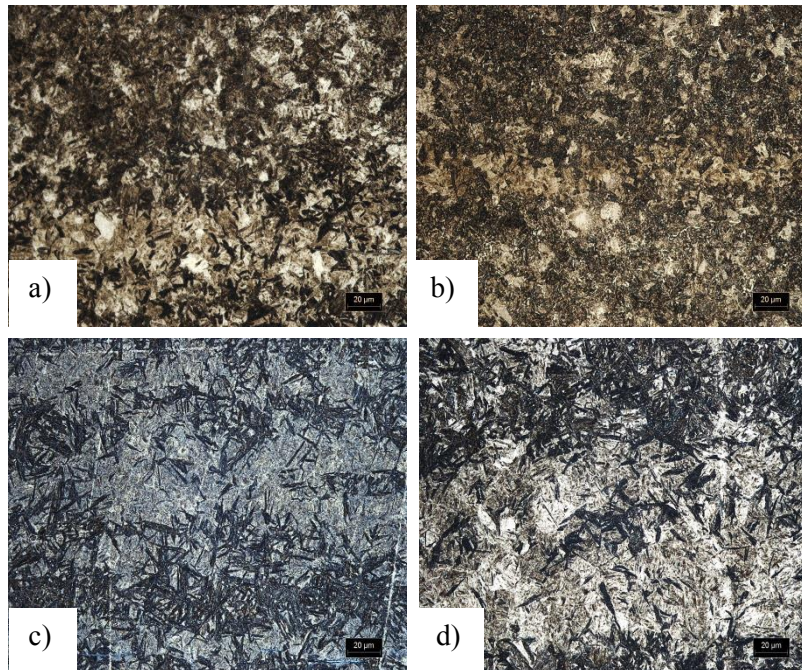


Figure 29. Representative images taken of the microstructures at x500 magnification after 60 s, a) 326 C 10mm b) 326 C 20mm, c) 326 F 10mm and d) 326 F 20mm. Isothermally heat treated for 60 s in 608F

The microstructure for material 326C is finer than for material 326F. This makes it easier to distinguish the structures from each other in material 326F, and can also be an influencing factor affecting the amount of formed lower bainite.

5.2.4. Comparison of data

2 sample T tests were done in order to see if there was any statistical difference between variations of parameters.

The first tests were done for Trial A, the test was done in order to study the martensite transformation because it was difficult to count and classify any other structural features in material 326C.

There was a significant difference between the two materials and a box plot of the %martensite for each material can be seen in Figure 30. The 95% CI is between 6.3-24% differences in martensite content between the two materials.

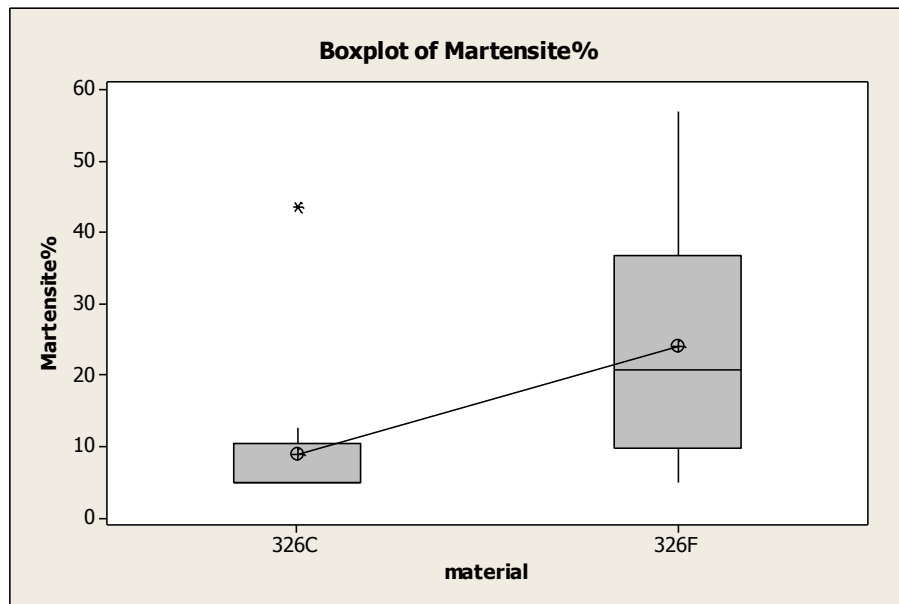


Figure 30. Box plot showing the difference in %martensite between material 326C and 326F

Same significant difference can be seen when studying the difference in macrohardness between the two materials, see Figure 31. Material 326F have approximately 1.4 HRC higher macrohardness than material 326C. The difference in macorhardness and in %martensite

supports each other, because it is reasonable to assume a higher hardness at higher martensite levels.

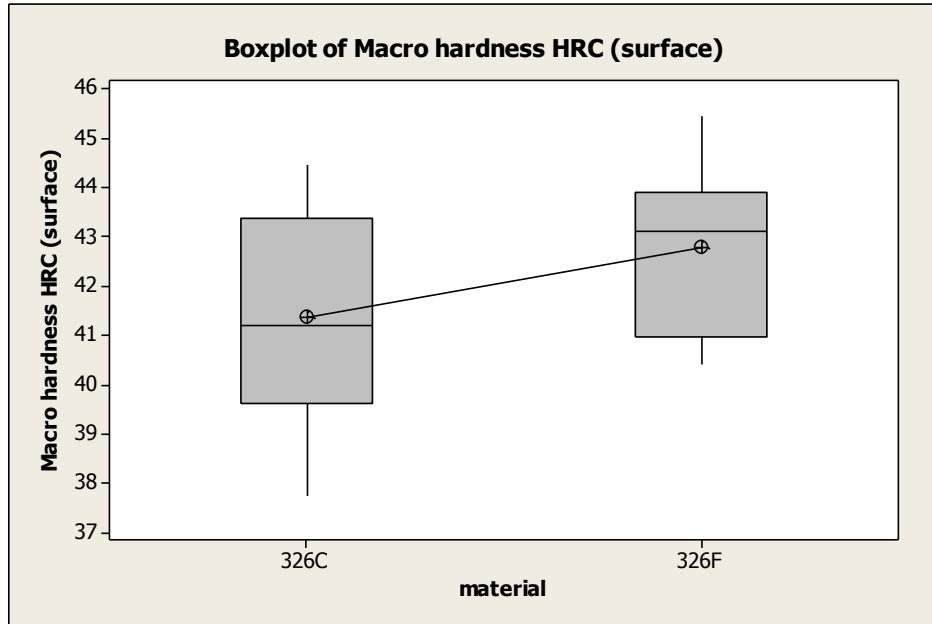


Figure 31. Box plot showing the difference in macrohardness between material 326C and 326F

Difference in microhardness for Trial A and B dependent on parameters such as: material, Time, thickness and orientation can be seen in Table 9. Also, difference in microhardness between the two trials can be seen in Table 9.

Table 9. 2 sample T and one way anova tests to compare different parameters with each other see if there was any statistical difference in microhardness.

<i>Difference in Microhardness (HRC)</i>					<i>Mean Microhardness (HRC)</i>
	<i>Material(326C and 326F)</i>	<i>Time (s), (60,90 and 120s)</i>	<i>Thickness (10 and 20mm)</i>	<i>Radial variation, (surface, middle and core)</i>	
<i>Trial A</i>	No significant difference	90 s showed highest values, no significance difference between 60 and 120s	10mm > 20mm, 2,4 HRC average difference	Surface & middle > Core	46.2 ± 4
<i>Trial B</i>	No significant difference	90 s showed lowest values, no significance difference between 60 and 120s	10mm > 20mm, 1,2 HRC average difference	Surface & middle > Core	47.1 ± 3.1

There was a difference in microhardness between the both thicknesses in Trial A. Samples with 10mm thickness had in average 2,4HRC higher hardness than the 20mm thick samples. When comparing the different time isothermally heat treated, samples heat treated for 90 s had a higher hardness than the samples heat treated for 60 and 120 s. However, no significant difference could be seen between the two materials in Trial A.

There is a difference in macrohardness (surface hardness) in Trial A. However, no significant difference could be seen in microhardness from the surface to the core between the two materials.

The thinner samples had in average a 1,2HRC higher microhardness than the thicker samples in Trial B. When comparing the different time isothermally heat treated, samples heat treated for 90 s had a lower hardness than the samples heat treated for 60 and 120 s. However, no significant difference could be seen between the two materials in Trial A.

Samples in Trial B had in average higher hardness than samples in Trial A. This can be a result of the lower isothermal heat treating temperature in Trial B, together with the longer time immersed in water in after isothermal heat treating step in Trial B. It is therefore reasonable to think that lower temperature and faster quenching in water after isothermal heat treating result in higher hardness. The hardness of the martensite structure seems to be the controlling factor when it comes to the total hardness. While the lower bainite structure up to a 25-30% could lead to an increase in strength.

Material 326 F provides the best result when it comes to distinguish the lower bainite and martensite structures. The lower bainite content is less, due to the higher hardenability, and is therefore further studied.

Both heat treating trials performed in molten salt has been analyzed with respect to the bainite content. One assumption is that the darker etched areas are lower bainite, while the lighter colored areas are martensite This is based on the morphology of the constituents in the darker areas, due to the resemblance in appearance of the darker structure compared to earlier work. All etching methods were adopted from earlier work on the subject, and is further discussed in 5.3.

The result is presented in two sample groups, samples with 10 and 20mm in thickness respectively for material 326 F and can be seen in Figure 32 and Figure 33.

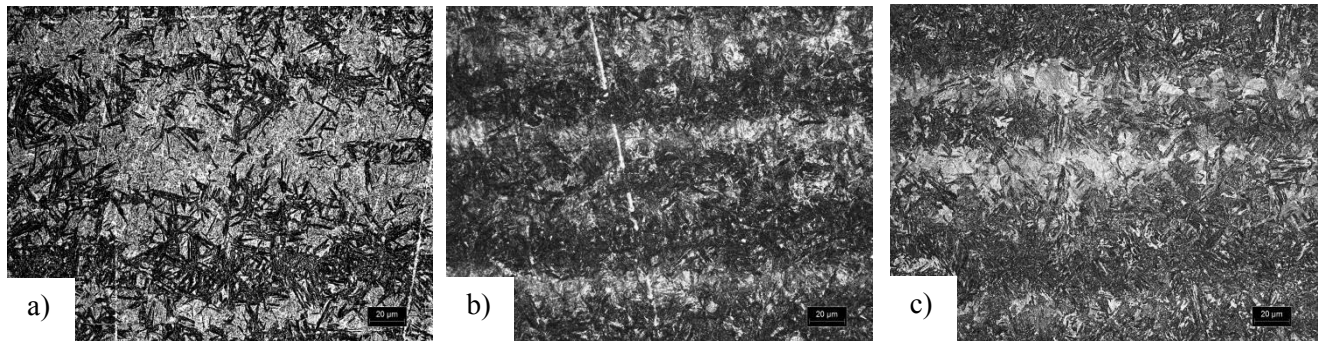


Figure 32. Samples studied with same material (326F) and thickness (10mm) but form different heat treatments, a) 61% lower bainite, austempering from Trial B at 60 s, b) 70% lower bainite, austempering from Trial A at 90 s and c) 85% lower bainite, austempering from Trial A at 120 s.

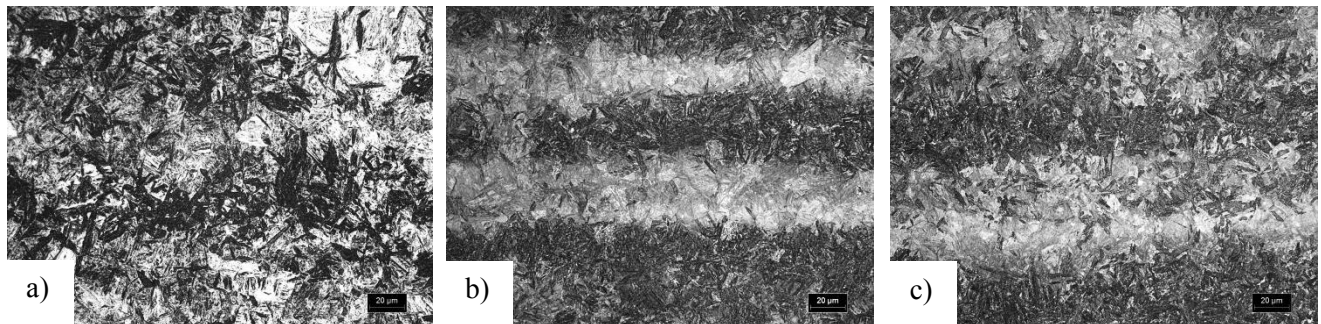


Figure 33. Samples studied with same material (326F) and thickness (20mm) but form different heat treatments a) 44% lower bainite, austempering from Trial B at 60 s b) 54% lower bainite, austempering from Trial A at 90 s and c) 77% lower bainite, austempering from Trial A at 120s.

The bainite content and the standard deviation can be seen in Table 10. It should be mentioned that more samples should be investigated to better pin point the bainite content for each heat treatment. There is no statistically significant difference between longer times isothermally heat

treated and increased lower bainite content. It is necessary to perform more tests and to collect and analyze more data, to better understand the influence of transformation temperature and time isothermally heat treated. Each value is an average of three samples and three different areas for each sample.

Table 10. Sample thickness and %Bainite and the related heat treatment, for material 326F

<i>Sample</i>	<i>% Bainite</i>	<i>Heat Treating</i>
<i>326F 10mm</i>	61 ± 6.93	Trial B, 60 s
<i>326F 10mm</i>	70 ± 19.6	Trial A, 90 s
<i>326F 10mm</i>	85 ± 9.23	Trial A, 120 s
<i>326F 20mm</i>	44 ± 3.61	Trial B, 60 s
<i>326F 20mm</i>	54 ± 10.38	Trial A, 90 s
<i>326F 20mm</i>	77 ± 13.75	Trial A, 120 s

The lower bainite needles seem to be finer in Trial B, and can be a result due to the lower transition temperature. Research has indicated that the lower bainite needles will not be provided with an increased thickness at longer transformation times. The needle thickness depends more on the transformation temperature, lower temperature provides thinner lower bainite needles. [18] It would therefore be interesting to further study even lower transformation temperatures, under the 320°C temperature tested in this work, for lower bainite formation. How far below the M_S is it possible to isothermally heat treat and still form lower bainite needles? Lower temperature could also help to increase hardness, due to increased quenching speed.

5.3. Etching methods

Different etching methods were tested in order to try to find a method to better distinguish the martensite and the lower bainite structure. Representative images of the different results can be seen in Figure 34. All four methods reveal the martensite and non-martensite features. However, some of the methods revealed more information. To choose etching method the results were compared to earlier work on etching martensite and bainite structures.

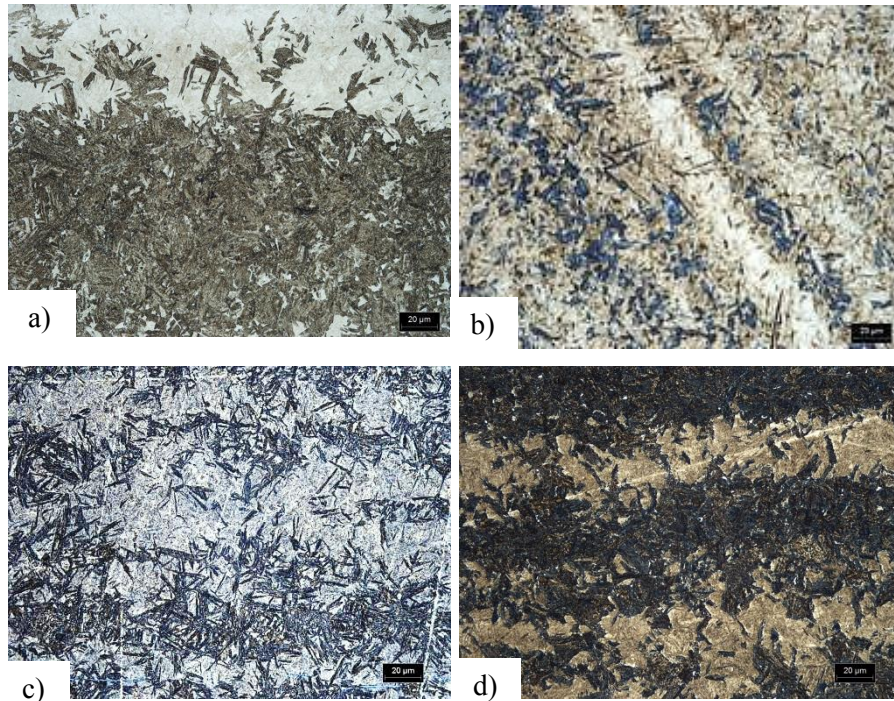


Figure 34. Variation of etching methods and chemicals: a) 2% Nital, b) 4% picral+ 1% Sodium Metabisulfite c) 4% Picral+HCl and d) 2% Nital and 5% Sodium Metabisulfite

From the work of Vander Vort [44] upper bainite and as-quenched martensite have been etched with sodium metabisulfite, and can be seen together with a picture of material 326F isothermally heat treated for 120 s, in Figure 35. The as-quenched martensite has been given a brown color, while the bainite and other non-martensitic transformation products, if any, have a dark blue color.

The variation of the structural features in the microstructure especially for material 326C, resulted in that the etching method with nital and sodium metabisulfite provided best results because it reveals most information of the microstructure, and etch lot of different features. The etching method used for both trials are selected depending on the etchants ability to distinguish martensite and non-martensitic transformation products. For Trial A Sodium metabisulfite provided the best result.

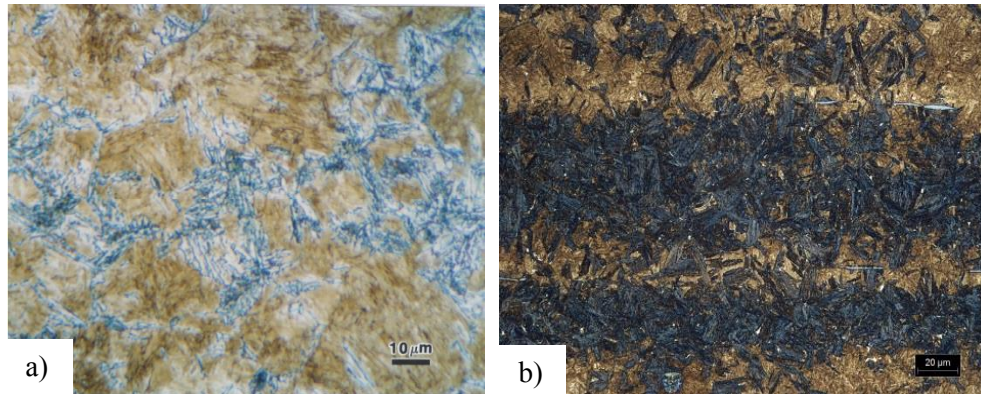


Figure 35. a) From the work of Vander Vort a microstructure upper bainite (blue) and as-quenched martensite (brown) etched with 10% sodium metabisulfite [44] b) material 326F etched first with nital and then with 5% sodium metabisulfite, structure of lower bainite (blue) and as-quenched martensite (brown).

In order to get best result etching the samples with sodium metabisulfite, the following steps should be considered:

1. 5g sodium metabisulfite powder and 100ml still water is mixed together, which provides a solution of approximately 5% sodium metabisulfite. Use a fresh mix at every etching occasion.
2. Etch a freshly polished surface in 2% Nital for 2-5s to remove possible oxide layer.
3. Etch the sample in the solution with 5% sodium metabisulfite in still-water in 30-60 s.
4. Put the sample in a crucible with water, do not rinse under running water. Rinsing under running water could destroy the deposited sulfide film.
5. Dry the same.

In Trial B the samples were tempered, the sodium metabisulfite method did not work as good for the tempered samples. Instead another method was used, consisting of picral and HCl. From the work of C.D Liu *et.al*, [2], pictures of mixed microstructure of bainite and martensite was etched with 4% picral and HCl. A comparison between their work and the result from Trial B where the same etching method was used can be seen in Figure 36. Trial B was tempered in order to level out the hardness profile and to produce tempered martensite. The picral and HCl solution showed best result for Trial B.

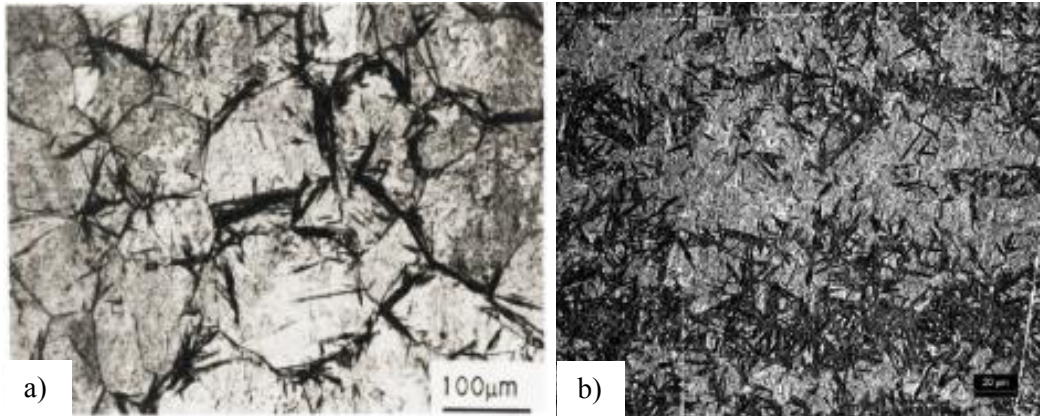


Figure 36. Comparison between the work of, a) C.D Liu *et.al*, [2], and b) the result from Trial B sample 326F 10mm after 60s. Both samples is etched in 4% Picral and HCl.

One step in the production of injector bodies at Cummins Fuel Systems is a tempering step. The tempering will result in tempered martensite. During the tempering fine dispersed carbides will precipitate inside the martensitic phase. The diffusion of carbon during tempering at elevated temperatures could result in a change of the martensite lattice parameters. This is further discussed in section 2.4. Both tempered martensite and lower bainite have precipitated carbides. But the distribution of carbides is different between the two structures. Even if the morphology of the ferrite needles in a matrix of martensite reveal the lower bainite structures. It is necessary to confirm the features in a SEM or TEM. The orientation of the precipitated carbides is different for tempered martensite and lower bainite, this specific orientation can be studied in TEM.

6. Conclusions

- 326F material shows less amount of lower bainite structure.
- Material 326F provides higher average surface hardness before tempering.
- It is possible to create a variation of lower bainite content in a matrix of martensite by interrupted isothermal heat treating in molten salt.
- It is possible to distinguish bainite from martensite under LOM depending on the etching methods.
- Lower transformation temperature result in thinner needles and higher average hardness.

7. Further work

- SEM or TEM to confirm bainitic and tempered martensitic constituents. Both structures have characteristic carbide orientation within each phase distinguishing them from each other.
- A more quantitative study of heat treatments around M_S to better understand the growth mechanisms. Test more isothermal heat treating temperatures to better control the lower bainite content.
- More etching methods should be tested, to better understand etching parameters *e.g.* time and concentration of chemicals.
- In order to further investigate the bainite content, one way would be to study the microstructure before tempering. As-quenched martensite does not have precipitated carbides.
- The work should be focused toward 326 F material from Ovako AB, because it's higher hardenability, which seems to result in slower lower bainite transformation.
- Perform XRD-analysis in order to see if any retained austenite is present in the microstructure. Retained austenite has impairing effects on the mechanical properties.
- EBSD- analysis to study the lower bainite refinement of the martensitic structure. This study could provide a better understanding of the refining effects of the lower bainite needles on the martensitic structure.

References

- [1] Y. Tomita and K. Okabayashi, *Heat treatment for improvement in lower temperature mechanical properties of 0.40 pct C-Cr-Mo Ultrahigh Strength Steel*. Metallurgical transactions V. 14A, Nov 1983 (2387-2393)
- [2] C.D. Liu and P.W. Kao, *Tensile properties of a 0.34C-3Ni-Cr-Mo-V steel with mixed lower-bainite-martensite structures*, Material Science and Engineering A150 (1992) 171-177
- [3] D.Y. Wei, J.L. Gu, H.S. Fang, B.Z. Bai, Z.G. Yang, *Fatigue behavior of 1500 MPa bainite/martensite duplex-phase high strength steel*, International Journal of Fatigue 26 (2004) 437-442
- [4] J. Chakraborty, I. Manna, *Development of ultrafine ferritic sheaves/plates in SAE 52100 steel for enhancement of strength by controlled thermomechanical processing*, Materials Science and Engineering A 548 (2012) 33-42
- [5] A. Abdollah-Zadeh*, A. Salemi, H. Assadi, *Mechanical behavior of CrMo steel with tempered martensite and ferrite-bainite-martensite microstructure*, Materials Science and Engineering A 483-484 (2008) 325-328
- [6] George Krauss, *Steel: Processes, Structure and Performance*, ASM International, ISBN: 0-87170-817-5, August 2005
- [7] G.E. Totten, G.E. Totten & Associates, LLC, M. Narazaki, Utsunomiya University (Japan), R.R. Blackwood and L.M. Jarvis, Tenaxol Inc., *Failures Related to Heat Treating Operations*
- [8] S. Morito, H. Yoshida, T.maki, X. Huang, *Effect of block size on the strength of lath martensite in low carbon steels*, Materials science and engineering A438-440 (2006) 237-240
- [9] S. Morito, X. Huang, T. Furuwara, T. Maki, N. Hansen, *The morphology and crystallography of lath martensite in alloy steels*, Acta Materialia 54 (2006) 5323–5331
- [10] Kangying Zhu, Olivier Bouaziz, Carla Oberbillig, Mingxin Huang, *An approach to define the effective lath size controlling yield strength of bainite*, Materials Science and Engineering A 527 (2010) 6614–6619
- [11] Parrish, Geoffrey, *Carburizing Microstructures and Properties*, ASM International, December 1990

- [12] Peter Kolmskog *Does Bainite form with or without diffusion? The experimental and theoretical evidence*, Kungliga Tekniska Hogskolan, ISBN: 978-91-7501-755-6, 24 may 2013
- [13] Zhi-Gang Yang , Hong-Sheng Fang, *An overview on bainite formation in steels*, Current Opinion in Solid State and Materials Science 9 (2005) 277–286
- [14] H. K. D. H. Bhadeshia, *Bainite in Steels - 2nd Edition*, Published by the Institute of Materials, Publication Date: 9 march 2001, IBSD: 1-86125-112-2
- [15] Mats Hillert, *Paradigm shift for bainite*, Scripta Materialia 47 (2002) 175–180
- [16] H. K. D. H. Bhadeshia, LOW–CARBON STEELS: THE CALCULATION OF MIXED–MICROSTRUCTURES & THEIR MECHANICAL PROPERTIES, University of Cambridge/Research and Development Corporation of Japan Department of Materials Science and Metallurgy Pembroke St., Cambridge CB2 3QZ, U. K.
- [17] Khodamorad Abbaszadeh, Hassan Saghaany and Shahram Kheirandish, *E@ect of Bainite Morphology on Mechanical Properties of the Mixed Bainite-martensite Microstructure in D6AC Steel*, J. Mater. Sci. Technol., 2012, 28(4), 336{342
- [18] Z. Ławrynowicz, *Transition from upper to lower bainite in Fe – C – Cr steel*, Materials Science and Technology November 2004 Vol. 20
- [19] J.W. Christian, *The Theory of Transformations in Metals and Alloys (Part I + II)*, Pergamon December 2002
- [20] Yoshiyuki Tomita, *Review: Morphology control of ductile second phase and improved mechanical properties in high strength low alloy steels with mixed structure*, Journal of materials science 27 (1992) 1705-1715
- [21] Yoshiyuki Tomita and Kunio Okabayashi, *Mechanical Propeties of 0.40 Pct C-Ni-Cr-Mo High Strength Steel Having a Mixed Structure of Martensite and Bainite*, Metal. Trans. A Volume 16A, January 1985 (73-82)
- [22] C.H young and H. K. D. H. Bhadeshia, *Strength of mixtures of bainite and martensite*, Mater. Sci. Technol. 10 (1994) 209-214
- [23] George E. Totten, *Steel Heat Treatment, Metallurgy and Technologies, Chapter 9 Quenching and Quenching, Technology*, by Hans M. Tensi, Anton Stich, and George E. Totten

- [24] H.-G. Lambers, S. Tschumak, H.J. Maier, D. Canadinc, *On the bainitic and martensitic phase transformation behavior and the mechanical properties of low alloy 51CrV4 steel*, International Journal Of Structural Changes In Solids, 3(2011) 15-27
- [25] H. Ohtani, S. Okaguchi, Y. Fujishiro and Y. Ohmori, *Morphology and Properties of Low-carbon Bainite*, Metal. Trans. A Volume 21A 1990 (877-888)
- [26] Kh. Abbaszadeh, Sh. Kheirandish, H. Saghafian, *The Effect of Lower Bainite Volume Fraction on Tensile and Impact Properties of D6AC Medium Carbon Low Alloy Ultrahigh Strength Steel*, Iranian Journal of Materials Science & Engineering Vol. 7, Number 3, Summer 2010
- [27] RICHARD FARRARA, Comparison of isothermal salt quench and oil quench plus temper of 4XXX low alloy steels, US Army Armament research, Development and Engineering Center close Combat armaments center Benet Laboratories Watervliet, N.Y. 12189-4050, Feb1996
- [28] A.H. Meysami, R. Ghasemzadeh , S.H. Seyedein, M.R. Aboutalebi, *An investigation on the microstructure and mechanical properties of direct-quenched and tempered AISI 4140 steel*, Materials and Design 31 (2010) 1570–1575
- [29] G.R. Speich and W.C. Leslie , *Tempering of steel*, Metallurgical transactions volume 3, p.1043-1054, May 1972
- [30] B.L. Bramfitt and J.G. Speer. *A perspective on the morphology of Bainite*, , Metallurgical Transactions A volume 21A p. 817-829, 1990 April.
- [31] V. García Navas, O. Gonzalo, I. Quintana, T. Pirling, *Residual stresses and structural changes generated at different steps of the manufacturing of gears: Effect of banded structures*, Material Science and Engineering A 528(2011) 5146-5157
- [32] <http://books.google.se/books?id=ibg3GWDxFRsC&lpg=PA28&ots=YsCaR7Gz mh&dq=segregation%20soaking%20homogenization&hl=sv&pg=PA34#v=onepage&q=segregation%20soaking%20homogenization&f=false>, 9:23 AM 4/28/2014
- [33] ASM International TTT, http://www.wpi.edu/Pubs/E-project/Available/E-project-020210-161513/unrestricted/JOMINY_END_QUENCHING_OF_4140_STEEL.2.pdf
- [34] Daniel H. Herring, *Oil Quenching*, <http://www.heattreatdoctor.com/documents/Vacuum%20Oil%20Quenching%20Tech.pdf> , 3/3/2014 3:05 pm
- [35] Gajen P. Dubal, *Salt bath quench*, Heatbath/Park metallurgical group, Detroit Michigan

- [36] S. Raygan, J. Rassizadehghani, and M. Askari, *Comparison of Microstructure and Surface Properties of AISI 1045 Steel After Quenching in Hot Alkaline Salt Bath and Oil*, 168—Volume 18(2) March 2009 Journal of Materials Engineering and Performance
- [37] Justin Lefevre and Kathy L. Hayrynen, *Austempered Materials for Powertrain Applications*, Journal of Materials Engineering and Performance, Volume 22(7) July 2013 (1914–1922)
- [38] S.M.C. Van Bohemen, M.J. Santofimia and J. Sietsma, *Experimental evidence for bainite formation below M_s In Fe-0.66C*, Scripta Materialia 58 (2008) 488-491
- [39] http://en.wikipedia.org/wiki/41xx_steel, 09:43 am, 3-3-2014
- [40] Harry Chandler (editor), *Heat theater's guide: Practices and procedures for Irons and steels*, ASM International ISBN 0-87170-520-6 (p. 319-325)
- [41] Josph R. Davis, *ASM Handbook: Volume 4 Heat Treating*, ISBN 0-87170-379-3
- [42] Bruce L. Bramfitt, Arlan O. Benschoter, *Metallographer's Guide: Practice and Procedures for Irons and Steels*, ASM International, March 2002
- [43] John E. Hilliard John W. Cahn, *An Evaluation of Procedures in Quantitative Metallography for Volume-Fraction Analysis*, TRANSACTIONS OF THE METALLURGICAL SOCIETY OF AIME, VOLUME 221, APRIL 1961 (344-352)
- [44] <http://www.georgevandervoort.com/metallography/general/iron-and-steel/20001270-microstructure-of-ferrous-alloys.html>, 1:34 PM 29/04/2014.